T.C.
İSTANBUL KÜLTÜR UNIVERSITY
INSTITUTE OF GRADUATE STUDIES

SEISMIC BEHAVIOR RC ADJACENT BUILDINGS DURING STRUCTURAL POUNDING WITH SOFT STOREY CONSIDERATION

Masters of Applied Science Thesis

ABDULLAHI MOHAMED ABDIRAHIM

1800004956

Department: Civil Engineering

Programme: Structural Engineering

Supervisor: Assist. Prof Dr. Erdal COŞKUN

JUNE 2021

T.C.
İSTANBUL KÜLTÜR UNIVERSITY
INSTITUTE OF GRADUATE STUDIES

SEISMIC BEHAVIOR RC ADJACENT BUILDINGS DURING STRUCTURAL POUNDING WITH SOFT STOREY CONSIDERATION

Masters of Applied Science Thesis

ABDULLAHI MOHAMED ABDIRAHIM

1800004956

Department: Civil Engineering

Program: Structural Engineering

Supervisor and Chairperson:
Assist. Prof Dr. Erdal COŞKUN

Members of Examining Committee:
Prof. Dr. Hüseyin Faruk KARADOĞAN
Assist. Prof Dr. Gökhan YAZICI

JUNE 2021

ACKNOWLEDGEMENT

First of all, I would like to thank ALLAH, who let to complete this work, and then to my dear supervisor Assist. Prof. Dr. Erdal COŞKUN, for his weariless, forgiveness, and upholding during this research work. Without him, I would not have been able to complete this task. He has relentlessly helped me incessantly, he has given me his precious time, and I will never forget how he encouraged me and ultimately led to my success.

Secondly, I would like to thank İstanbul Kültür University (IKU) for allowing me as one of their students and gave me this chance. Immensely I thank my department of Civil Engineering for finishing my master's degree.

I would also like to express my sincere thanks to my dear family. First, my dear beloved mother Amina Said and my brothers and sister supported me as encouraging and financing without interrupting me during my studies. Finally, I would like to thank all of my friends and colleagues and the Republic of Turkey for facilitating our studies in their country.

University: İstanbul Kültür University
Institute: Institute of Graduate Studies
Department: Civil Engineering
Programmed: Structural Engineering
Supervisor: Assist. Prof. Dr. Erdal COŞKUN

ABSTRACT

In the recent past earthquakes, several poundings of adjacent structures have been observed severe damages; even some of them collapsed totally. Several researchers have been focused on this phenomenon to reach a suitable solution to prevent the structure from pounding damages during an earthquake. In this book, 2D of RC adjacent building with infill wall and without infill wall of nine and six-story have been modeled under five different ground motions with various PGA and Mw have been subjected to the adjacent buildings by SAP2000. V21.

The ground motions have been selected from the PEER ground motion database and then scaled by the Seismo-Macht program by matching the target response spectrum obtained from standard TSC18. Nonlinear elastic modeling with 0.5mm gap separation has been simulated to calculate the pounding force. Nonlinear time history analysis with a direct integration as a type of solution has been taken to obtain model results. SAP2000 V21 has been performed to carry out the analysis of all models. The seismic effect of pounding on the adjacent buildings with infill walls and without infill walls has been considered during earthquake excitation. The results have been shown in the form of story displacement, story drift ratio, pounding force, acceleration, and pounding history.

The results from both cases are compared to determine which one has a critical seismic effect. The seismic behavior of pounding adjacent buildings is significant. Whenever; The dynamic difference between adjacent buildings increases, the pounding force, and acceleration increase while the displacement decreases.

Üniversite: İstanbul Kültür Üniversitesi

Enstitüsü: Lisansüstü Eğitim Enstitüsü

Anabilim Dalı: İnşaat Mühendisliği

Programı: Yapı (İngilizce)

Tez Danışmanı: Assist. Prof. Dr. Erdal Coşkun

ÖZET

Yakın geçmişte meydana gelen depremlerde, bitişik nizam yapıların çarpışmasında şiddetli hasarlar gözlenmiş, hatta bazıları çökmüştür. Yapının deprem sırasında hasar görmesini önlemek ve uygun bir çözüme ulaşmak için birçok araştırmacı bu soruna odaklanmıştır. Bu çalışmada, betonarme ve dokuz ve altı katlı dolgu duvarı olmayan betonarme bitişik nizam bina çerçevelerinin çeşitli PGA ve M_w ile beş farklı deprem hareketi için modellenerek SAP2000 V21 ile bitişik nizam yapıların davranışı incelenmiştir.

Yer hareketleri, PEER yer hareketi veri tabanından seçilerek ve ardından TSC18'den elde edilen hedef tepki spektrumu ile eşleştirilerek Seismomatch programı ile de ölçeklendirilmiştir. Çarpma kuvvetini hesaplamak için 0,5 mm boşluklu doğrusal olmayan elastik modelleme simüle edilmiştir. Model sonuçlarını elde etmek için bir çözüm türü olarak doğrudan entegrasyonlu doğrusal olmayan zaman tanım alanı analizi yapılmıştır.

Tüm modellerin analizini gerçekleştirmek için SAP2000 V21 yazılımı kullanılmıştır. Deprem sırasında, dolgu duvarı olan ve dolgu duvarı olmayan bitişik binalarda çarpmanın sismik etkisi dikkate alınmıştır. Sonuçlar, kat yer değiştirme, kat kayma oranı, çarpma kuvveti, ivme ve çarpma geçmişi şeklinde gösterilmiştir. Her iki durumda da elde edilen sonuçlar, hangisinin kritik sismik etkiye sahip olduğunu belirlemek için karşılaştırılmıştır.

Bitişik binalar arasındaki dinamik fark artınca, yer değiştirme azalır çarpma kuvveti ve ivme artar.

Anahtar Kelimeler: Çarpma kuvveti, bitişik nizam, boşluklar, boş çerçeve, dolgu duvar.

Table of Contents

LIST OF FIGURES

LIST OF TABLES

LIST OF ABBREVIATIONS

ASCE: American Society Of Civil Engineers

TSC18: Turkish Seismic Code 2018

CBD: Christchurch Central Business District

RC: Reinforced Concrete

2D: Two Dimensions

RB: Right Side Building

LB: Left Side Building

SDOF: Single Degree Of Freedom

MDOF: Multiple Degree Of Freedom

UBC: Uniform Building Code

PGA: Peak Ground Acceleration

TBC: T*aiwan* Building Code

ABS: Absolute Sum Method

SRSS: Square Root Of The Sum Of The Squares

DDC: Double Difference Combination

LVM: Linear Viscoelastic Model

MLVM: Modified Linear Viscoelastic Model

Nlvm: Nonlinear Viscoelastic Model

HDM: Hertz Damp Model

HCM: Linear Hunt-Crossley Model

NE: Normalized Error

SSI: Soil Structural Interaction

THA: Time History Analysis

IBC: Uniform Building Code

LS: Left-Side Direction

RS: Right-Side Direction

CPG: Cerro Prieto Geothermal

WES: Westside Elementary School

LIST OF SYMBOLS

퓰= Parameter of correlation

T_L, T_R= Natural period of left and right-side buildings

퓸퓲=Damping ratio of *i*-structure

퐦퓲= Mass of i-structure

퐦퓵, 퐦퓻 = Mass of first building, and mass of second building

퐦퓵 퐦퓻= Mass of first building, and mass of second building

D=Gap separation distance

흃퓵 , 흃퓻 = Damping ratio of first and second buildings, respectively

E=Coefficient of restitution

K=Impact stiffness (linear parameter)

K=Impact stiffness (nonlinear parameter)

퓬= damping coeficient

u_i= peak response displacement of i-structure

Q=Live load

G=Dead load

W=wall load

EX=Earthquake load at X-direction

S_S= the mapped MCE_R spectral response acceleration parameter at short periods

S_1= the mapped MCE_R spectral response acceleration parameter at a period of 1s

M= Mass coefficient matrix

C=Damping coefficient matrix

K= Stiffness coefficient matrix

F(t)= external load vector

퐅=pounding force

퓾= Acceleration vectors

퓿= Velocity vectors

풖= Displacement vectors

휸= Gamma Coefficient

휷= Betta Coefficient

퓿퓲=initial velocity for i-element

퓿퓲′=final velocity for i-element

풉=height of dropping ball

풉′=height of rebound height measuring

푬퓲=modulus of elasticity for i-material

푬퓲퓷퓯= modulus of elasticity for infill wall material

푬퓯= modulus of elasticity for frame element material

풉퓲퓷퓯=height of infill wall

흀퓱=strut diagonal coefficient

퓽= strut diagonal thickness

퓭=strut diagonal length

퓵퓲퓷퓯=infill wall length

퓵퓫퓮=beam length

휽=slope of diagonal strut

CHAPTER 1

INTRODUCTION

1.1 General

Many adjacent structures have been built without having enough gap separation in the metropolitan cities because of financial and architecture issues. Being adjacent to closeness building and out of phase vibration, they collide during an earthquake. The collision of adjacent structures or some building parts during an earthquake or other lateral loads is called seismic induced pounding. Therefore, pounding might cause damage or collapse of building totally.

Most of the damage caused by the previous earthquake occurred to the masonry and concrete structures. Although the requirement of seismic separation was introduced later, most old buildings were built in narrow or null gap separation without considered seismic separation, particularly built-in seismic active regions. The pounding phenomenon increases when the adjacent buildings have a different natural period, and insufficient separation causes them to vibrate in the other direction, as reported [1].

For summarizing, the pounding phenomenon increases when each adjacent building has different dynamic properties and short gap separation distance, as in Figure 1.1. In this study, two adjacent buildings with various configurations under various horizontal ground motions are studied. The TSC-18 code has been considered during this study.

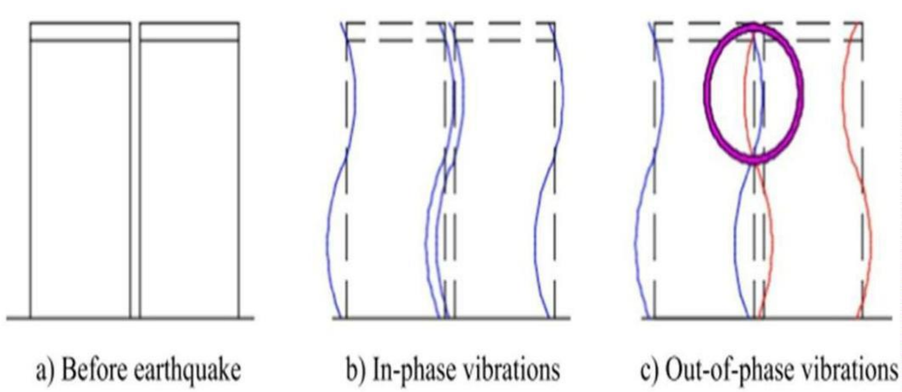

Figure 1.1: Dynamic behavior for neighboring buildings [1].

1.2 Factors that Create Pounding

In this section, the factors that cause the pounding of the adjacent buildings have been presented. Some of the factors related to the increased pounding of adjacent structures during earthquakes might exist. Many studies, articles, research, projects, and code requirements were recorded, which are the different influences that create the pounding events. These factors are included: (a) soil condition, (b) building heights, (c) story's height, (d) relative difference between adjacent buildings height, (e) separation between adjacent buildings, (f) lateral loads resistance system (g) impact's area surface (h) peak ground acceleration, (i) fundamental natural period, (j) the basic material construction such as (concrete, steel, masonry, etc.), (k) properties of dynamic, (l) lateral eccentricity, etc. [2].

1.3 Historical Observation Events

This section's main significant objectives are to preview the damages or failure to the adjacent structures after earthquakes due to the pounding. The Observations include some historical events related to the damages caused by pounding adjacent buildings under earthquake excitation those collected from all over the world.

1.3.1 Worldwide Pounding Events

In the Mexico earthquake (1985) the effect was estimated that about 10,000 people lost their life, 50,000 was Injured and 250,000 became homeless. Further, the economic crisis about $4000 million value of damage, about US$275 million (7%) was insured, more than 40% of buildings were collapsed or have big cracks, nearby 15% of these buildings had significant damage or total collapse. Some notes showed that 20-30% of this damage was caused by pounding [3, 4], as shown in Figure 1.2.

Figure 1.2: Pounding damages of adjacent buildings during the Mexico earthquake (1985) [4].

In the Loma Prieta earthquake (1989), the observation included more than 200 pounding cases out of over 500 buildings. San Francisco, Oakland, Santa Cruz, and Watsonville were affected by the Loma Prieta earthquake, building damages have been observed during pounding between adjacent structures. For the Loma Prieta earthquake, different factors to the pounding events are registered, such as construction type, ground acceleration, soil type, and separation between adjacent buildings. Different types of damages were recorded: failure of masonry, falling of a brick veneer, replacing fire protection water line, and architectural and structural damage [5].

In the Chi-Chi earthquake (1999) in Taiwan was recorded that 2,437 people died, while over 11,305 people were injured, and more than 107,002 people were becoming homeless. After an earthquake, the pounding events were observed. As shown in Figure 1.3a-d, the different samples from seismic pounding caused a short separation distance between adjacent structures from other places in Taiwan [6].

(a) Buildings with no separation

(b) Collapse building due to pounding

(b) Major damage due to pounding

(c) Minor damage due to pounding

Figure 1.3: Pounding damage due to small gap separation distance [6].

An earthquake had 7.9 Richter happened in Wenchuan in 2008 China. An investigation was raised in an area with overpopulation density to determine the number of harms produced from the Wenchuan earthquake (2008). General data related to harm caused by an earthquake (2008) shows that more than 69,000people were lost, 374,171 people were injured, over 15 million persons were displaced, and 5millions were becoming homeless.

The most significant reason which causes the damages was pounding between adjacent buildings, as some evidence reported. In Chengdu, especially in the business place (market), several buildings with more than 3-floors and a short separation distance between the adjacent buildings were recorded pounding damages. A high level of damages due to pounding was observed during this earthquake. Figure 1.4 shows the type of damages and their categories [7].

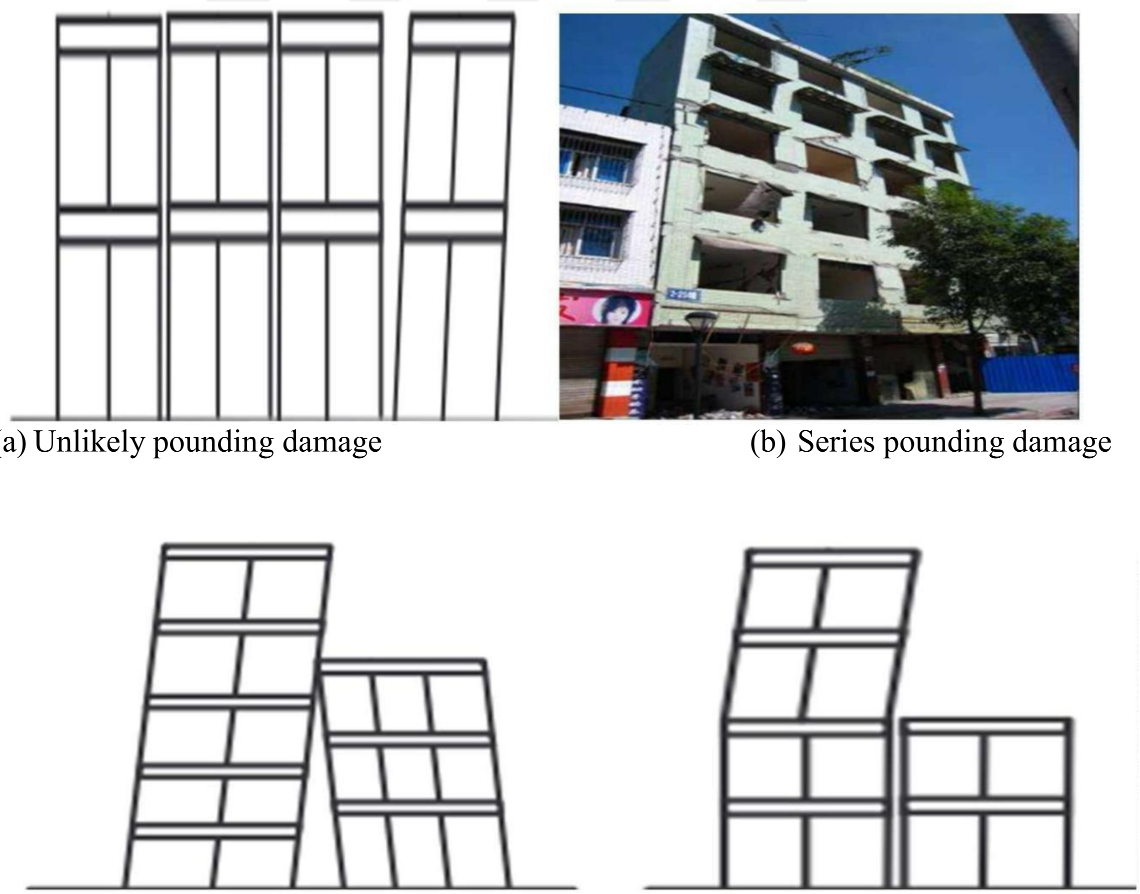

(a) Unlikely pounding damage

(b) Series pounding damage

(c) Column-floor pounding.

(d) Taller-shorter pounding

Figure 1.4: Building damages in the market area and the types of pounding [7].

In the Darfield earthquake (2010), pounding damage was observed in Christchurch's central business district (CBD). Small cracks were observed due to pounding buildings after five days. Unless some moderate damages were noted in some unreinforced masonry buildings, and also one story was collapsed due to pounding. In the CBD, some buildings were damaged by pounding. The estimation was recorded 5% of the structural damage from pounding buildings as in Figures 1.5. Finally, the building damages caused by the pounding become dangerous sources for future severe earthquakes in New Zealand [8].

(a) Pounding causes damage on 2nd story (b) Magnification of damage location(a).

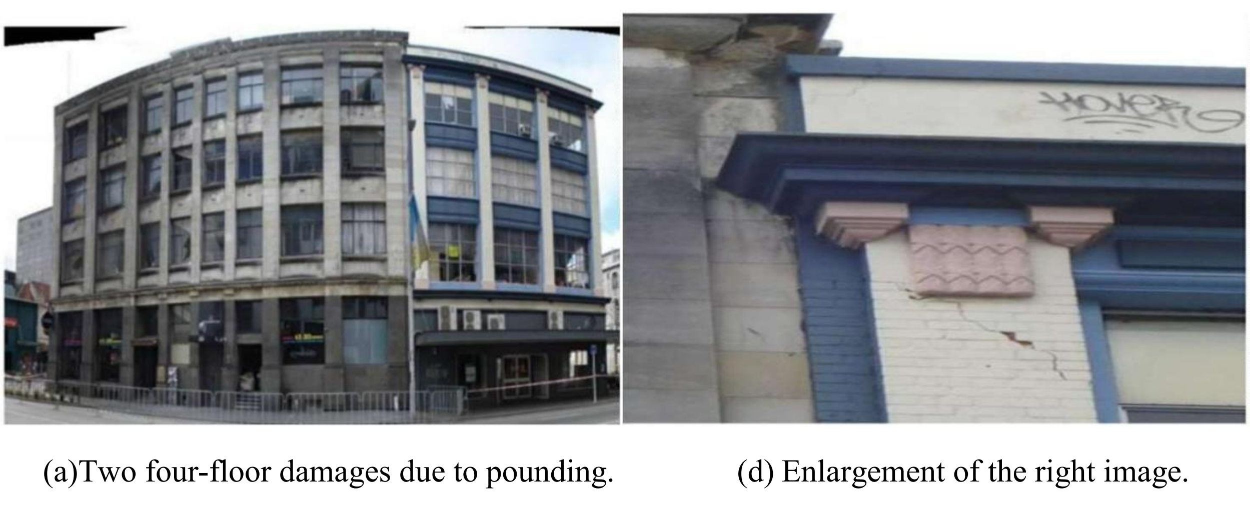

(a)Two four-floor damages due to pounding. (d) Enlargement of the right image.

Figure 1.5: Different types of pounding damages in the CBD [8].

The Lorca earthquake (2011) caused enormous harm such as fatalities, injured people, building damages, and economic collapse. The estimation has been illustrated that the epicenter distance was 5.5 km only from the epicenter. Two types of pounding have been recorded and observed during the Lorca earthquake (2011) [9], as shown in Figure 1.6:

(a) Masonry damage due to the pounding. (b) Floor-column pounding damage

Figure 1.6: Building damages during the Lorca earthquake (2011) [9].

1.3.2 Pounding Events in Turkey

Turkey is one of the most seismic regions globally. It also locates too critical a collision zone between the Eurasian plate. It happens between African and Arabian plates. However, Turkey has different hazard seismic zones, as shown in Figure 1.7. Therefore, the damages due to pounding under earthquake excitation are recorded. Some of the damaged buildings due to pounding effects are as follows.

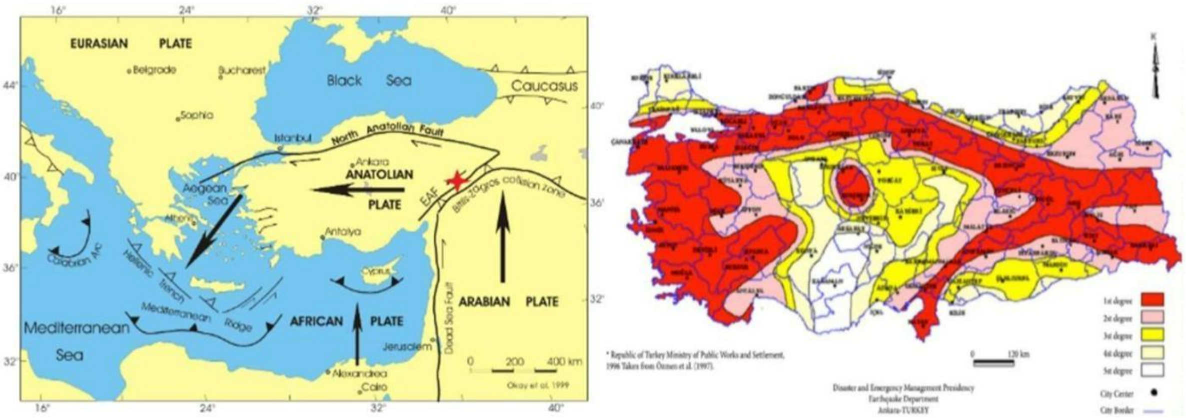

(a)Turkish tectonic boundary plate (b) Turkish different seismic zones (former seismic code)

Figure 1.7: Specification of Turkey boundary plates and its seismic zone [10].

On May 19, 2011, an earthquake hit Turkey, especially in Simav, Kütahya. It caused various levels of damage to the buildings due to different reasons. Pounding is the one of reasons which caused the injuries to the building during the earthquakes. In Simav city at Fatih district, pounding to five stories neighboring buildings with a small separation distance and inside damage in the building were observed during the examination due to pounding [11], as in Figure 1.8.

(a) Small damage due to pounding (b) Interior damage on the column during pounding

Figure 1.8: Outside and inside damages due to pounding during the earthquake in Simav [11].

The Tabanlı-Van earthquake (2011) had caused damages in the spread region in the Van district. Adjacent building pounding was observed as one of the joint structural damage. In the big streets of Van and Erciş, injuries of adjacent buildings constructed without separation distance were recorded [12], as in Figure 1.9.

(a) Van buildings affected by pounding (b) Ercis buildings affected by pounding

Figure 1.9: Adjacent buildings damaged due to pounding in (a) Van and (b) Erciş [12].

1.4 Scope of the Study

This study presents 2D reinforced concrete (RC) frame adjacent buildings with and without infill walls under different ground motions. The buildings are located side-by-side in the same line, which is called adjacent buildings. The adjacent buildings consist of two buildings: The left-side building (LB) and the right-side building (RB). Nine and six-story adjacent buildings have been considered in the study for both cases. The nonlinear elastic model with a gap separation of 0.5mm is respected to calculate pounding force.

Five different horizontal ground motions are obtained from PEER Ground Motion Database as pre-scaled form and also matched with the target response spectrum under standard TSC18 by using Seismomatch software.

Non-linear time history analysis with five horizontal ground motions has been used inside SAP2000 v.21 software. Finally, the base buildings are considered to be fixed bases during this study, where the soil interaction is ignored.

1.5 Objective of the Study

This study's objective is to assess the effect of pounding between adjacent buildings with various ground motions. The structural response results with five horizontal ground motions are compared to determine the most effective. Different horizontal ground motions are selected to perceive how the effect is different. The structural results include several responses such as (1) Story displacement, (2) Story drift ratio, (3) Pounding force, (4) Acceleration, and (5) pounding force of time history. The structural response results present as tables and graphs to understand the seismic behavior of pounding buildings. Finally, the results of both cases are compared to determine which condition will have the highest impact. This comparison will pave the way for a permanent solution or find a partial solution to decrease the pounding effect by respect three from five horizontal ground motions.

1.6 Arrangement of Thesis

The form of the thesis is an arrangement of six chapters, and the detail of each chapter is presented as below: -

Chapter one: concerns the Introduction of the thesis: general information related to the topic, factors that influence the pounding of buildings, the historical events in the world, the scope of the study, and objectives of the study.

Chapter two: collects several literature reviews related to pounding adjacent buildings, such as the analytical, experimental, and numerical studies.

Chapter three: summarizes the theoretical background related to the pounding adjacent buildings such as types of pounding, impact model, infill wall models, and review of analysis method.

Chapter four: expands modeling of pounding adjacent buildings, which applied to different horizontal ground motions: Modeling of the adjacent building, and input ground motions. It also discussed the scaling form, review of the analysis method, and the step-by-step modeling inside the SAP200 V.21 program.

Chapter five: presents the analysis result and discussion: First, the discussion of the structural response in adjacent buildings with and without infill wall under five horizontal ground motions was presented. Finally, comparisons of results from both cases are discussed in detail.

Chapter six: concluded the study's summary, conclusion, and future orientations.

CHAPTER 2

LITERATURE REVIEW

2.1 General

Unsuitable execution and many damaged buildings during past earthquakes because of the various adjacent structures built with no suitable separation distance between them or null. To realize the effect of pounding adjacent buildings in RC under the seismic influence. Several researchers and academicians have thought that the adjacent structures in diverse ways. The collision between adjacent structures during an earthquake is a phenomenon that many researchers have made. Most researchers, academics utilize to study this phenomenon by moderate numerical studies of single-degree of freedom (SDOF) and multi-degree of freedom (MDOF) systems to determine the problem and focus on the satisfactory solution. The literature review in the study offered will assort into the below:

- Analytical studies
- Experimental studies
- Numerical studies

2.2 Analytical Studies

Lin and Weng (2001) studied the evaluation of the seismic pounding hazard of adjacent buildings by the minimum separation requirement of UBC'97 during a specific period duration. Different 1000 artificial earthquakes for dynamic analysis with various PGA are studied. Multiple degrees of freedom (MDOF) system has 36 cases, 4 cases for building RB, and 9-cases for left building (LB). Comparisons of separation distance from study and those from UBC'97; The time-period of LB is vital while RB is specified. When both periods are close to each other (the ratio between them is approaching 1.0), it reveals the minimum code-required separation distances between adjacent buildings. The pounding probability of adjacent structures is decreasing very fast with the period ratio. The likelihood of 2.7% is the highest of the adjacent buildings. The pounding probability building (10%) that the ground motion of design basis in UBC'97 will overtake through 50years period [13].

Lin and Weng (2002) investigated the seismic pounding probability of buildings in the Taipei metropolitan area. About 1000 artificial earthquakes with different PGA have been taken. About 36-cases of adjacent structures contain 6-cases of RB, and 9-cases of LB are modeled. The separation building results obtained throughout the TBC'97 code compared those from the UBC'94 code to avoid the collision. Whenever the natural period of adjacent buildings is closed, the cross-correlation was ignored in TBC's method. The probabilities of the pounding are varying with the period of LB. The process of TBC has no similar risk for other cases. The most risk case revealed that the probability pounding received from both of TBC97's and UBC94's methods is 1.2% and 7%. According to the economy, UBC'97 is more satisfying than TBC'94 and will override the design basis of ground motions during 50-years is assessed at about 10% [6].

Garcia (2004) proposed a new method to calculate the critical separation distances between adjacent buildings. Two of single degrees of freedom (SDOF), he utilized non-linear time history hysteretic. The new method is based on examining the correlation parameter using Filiatrault, Penzien, Kasai, and Valles. The results were described by the ratio of minimum separation distances and peak relative displacement response. The result is shown from this study when compared to other methods (1) it always remains conservative (2) most cases; the conservative state is small (3) when the state of the conservative is not ignored, in addition to those results are less than those from other methods (i.e., ABS, and SRSS rules). The results of S from this study are not valuable for stopping pounding while land usage is for the minimum. None of the four methods provide a good standard. However, an examination shall be continuing to find adequate results for the DDC rule. The disadvantage of this study (DDC) that the parameters (p) were obtained from the chart [14].

Khatami, et al., (2019) proposed a new method for elastic and inelastic structures to prevent the collision between adjacent buildings. Six different models of adjacent buildings with unlike stories under three various ground motions were modeled. The CRVK of the computer program was used to cover this study. For elastic structure, they conducted the ABS, SRSS, Jeng, et al., and Nader pours et al. method were used. For the inelastic buildings, Penzien and Kasai et al. were used. The result was conducted of three and seven stories of adjacent buildings for both elastic and inelastic behaviors. In the elastic-buildings, the results SRSS and Naderpour et al. have optimal minimum separation to stop the collision of adjacent buildings while the other two rules (ABS and Jeng et al.) hard to agree on suggested separation distance more than the required due to financial issues. Furthermore, the inelastic buildings found that the proposed method of the periods has been the most interesting one when the buildings are considered the inelastic case. It allows us to stop the pounding of adjacent structures during an earthquake by providing appropriate separation distance between the neighboring buildings. The only disadvantage of this study is that the value of the separation distance obtained from charts [15].

2.3 Experimental Studies

Khatiwada, et al., (2013) tested pounding force between two hung reinforced concrete slabs, and each one had sizes 550 x 550 x 120 mm, each one hung on the top of two cables. Two laser sensor equipment are put on both sides (left and right sides) to measure the displacement between the ends of the slabs. However, two accelerometers are placed under each table to register the acceleration of the slab. The contact dimension of the slab has a size of 100 x 550 x 120 mm, and the center of the surface seems like a curve of 100m diameter. Five different numerical viscoelastic force models:

- Linear viscoelastic model (LVM).
- Modified linear viscoelastic model (MLVM).
- Nonlinear viscoelastic model (NlVM).
- Updated Hertz damp model (HDM).

Linear Hunt-Crossley model (LHCM)

To be part of the test to evaluate the pounding force and then compared with the one obtained from experimental. The results were obtained from five numerical viscoelastic models compared to those obtained from the experiment were compared to ensure the number of errors. The results have shown that peak pounding force from the numerical model was equal to one obtained from the experimental when the velocity is 0.096 m/s. for both cases. To ensure the amount of error of pounding force calculated from the five numerical viscoelastic models using the normalized error (NE). Both the LHCM and NIVM models are defined perfectly. The LVM and NIVM models are verified as accurate. Finally, the HDM model had the lowest error, while the MLVM has the highest error in all other models (Sushil Khatiwada, Nawawi Chouw, and Tam Larkin, 2013) [16].

Jankowski, et al., (2015) tested the adjacent pounding structures under earthquake. Two models with different configurations. Both models had three series shaking tables with five ground motions and with varying separations of the gap. For the first configuration, they used one rigid tower and two flexible ones, where they placed the rigid one in the middle and the other at the sides (left and right). For the second configuration, they used one flexible and two rigid towers, where they put the flexible one in the middle and placed the others at the sides (left and right). The results showed that the shape of time-vs-acceleration is similar in general unless at the point of 5sec. The pounding and non-pounding were compared. The ratio between peak acceleration of the pounding case to the non-pounding case is 1.35 for the first configuration, while 0.05 for the second configuration. The results showed that the structural properties (rigid & flexible) have been affected by pounding where the rigid tower of the first configuration has more acceleration response than the second configuration. Finally, increasing and decreasing the gap distance causes an increasing or decreasing acceleration, respectively [17].

Sołtysika, et al., (2017) tested the effectiveness of the polymer materials, which placed between adjacent structures to prevent the impact during an earthquake. Three (SDOF) steel towers under two ground motions (El Centro & Kobe). The structural bracing was used to Prevent the structure from torsion, and the concrete plate was placed on the external towers. The gap separation distance between the towers of 40mm with different size thicknesses of polymer materials: 10mm, 20mm, 30mm, and 40mm are considered. The state of adjacent steel towers having polymer materials compared to those not have polymer material. The results showed the thickness of polymer material has a significant effect because it causes to reduce the acceleration when it increases. Placing polymer materials between structures can be used to prevent buildings from colliding during an earthquake as a mitigation technique [18]

Jankowski (2010) studied two experiments regarding the different building materials, such as steel, concrete, timber, and ceramic. The first test has taken place by dropping balls with various masses onto a rigid plate surface of the same material and recorded prior-impact velocity using the B&K type-4344 accelerometer. The second one has consisted of two adjacent shaking tables under El Centro Earthquake. Supported elements and bracing elements are different in mass and cross-section for left and right-side towers. Two ENDEVCO-type 7752 accelerometers were connected to the towers to evaluate the response time histories during the test. The result was shown that the highest response and lowest response were shown from ceramic balls and timber balls, respectively. Increasing restitution coefficient leads to a decrease in the prior-impact velocity in the first test. Also, the second one has shown that the left tower has higher response values than the right ones in all different materials. The response increases 4.9% when steel to steel impact, while it increases 0.4% only when timber to timber impact [19].

Shrestha, et al., (2014) tested two bridges under different ground motions with mitigation equipment. Two bridge models with 50m size placed on the two adjacent shake tables under five ground motions from three soil classes whose PGA are in between 0.15 g-0.9 g were considered. The researchers tested the adjacent bridges with mitigation equipment and adjacent bridge without mitigation equipment. The result showed that the fixed foundation bridge was damaged more cracks than with a rocking foundation [20].

Lou, et al., (2018) experimented with the most accurate separation distance between buildings. Ten and six-story RC frame adjacent buildings using Open Sees Software for Simulated and Two and three-story shaking tables for experimental have been considered under 10-20 ground motions. The results from Open Sees compared to those of the experimental one. The vulnerability curves from the testing and those from the Open Sees model are similar when expressed in all cases. Finally, the study has shown that the results obtained from the numerical simulated Open-Sees are more accurate than those obtained from the experimental. It is also similar to the actual structure response [21].

Guo, et al., (2008) tested the effect of pounding adjacent structural highway bridges. They placed two slabs on the two adjoining shaking tables under three different ground motions. Pounding and non-pounding states are compared under various ground motions to see how their behavior difference. The acceleration increased higher than the non-pounding case. A pounding case has more significant than a non-pounding [22].

2.4 Numerical Studies

All degrees of freedom are essential for structural analysis. The horizontal, vertical, and rotational are necessary to analyze structures. However, the horizontal degree of freedom is primarily have been considered and ignored the vertical and rotational. Therefore, the numerical study of the horizontal degree of freedom has been classified into two classes (1) Single degree of freedom (SDOF) and (2) Multiple degrees of freedom (MDOF).

2.4.1 Single Degree of Freedom (SDOF)

Jankowski (2005) studied the impact force spectrum for damage assessment of earthquake-induced structural pounding. Two (SDOF) adjacent buildings with insufficient separation have been conducted. The non-linear viscoelas9tic model is considered to accounts for the energy dissipation during impact. The researcher investigated the effect of the different parameters on the impact force spectrum, which different masses, different values of damping ratio, and various gaps.

The results showed that the shape of the spectrum is associated with the input ground motion. The increasing damping ratio leads to reduce the impact force. Increasing mass causes to increase in the impact force and Increasing gap size leads to a decrease in the pounding force. The building located on the right side is assumed to be new, where the left one is assumed to be old [23].

Jankowski (2006) studied the pounding force response spectrum under earthquake excitation. In this study, single degrees of freedom for both buildings were selected. The nonlinear viscoelastic model was considered as a gap connection. Several different dynamic parameters were studied to determine their effects on the impact force. The various parameters include masses, damping ratios, gap sizes, and time lag. For the elastic structure, the pounding force was decreased with increased damping ratios by 0-2% of two buildings simultaneously. However, the pounding force is equal to zero at the extension of the region in the spectrum. The pounding force increasing rapidly when the masses increasing. The pounding force does not change more for the rate change of time lag (0.2s-0.5s). For inelastic structure, the pounding force did not change as change the ductility of the right-side building where the left one was kept constant. However, the pounding force reduced when the ductility for both adjacent building increase [24].

Naderpour, et al., (2016) studied the numerical study pounding between Two Adjacent Buildings under earthquake excitation. In the study, adjacent buildings were modeled as a single degree of freedom were selected. The nonlinear viscoelastic model was used to calculate pounding force. Four different ground motions with having different PGA were used. Nonlinear time history analysis was done by using Open-Sees. The study has been examined various parameters with different values. The result showed that the impact force depended basically on the earthquake excitation. Furthermore, the peak impact during contact is related to gap size, restitution coefficient, impact velocity, and stiffness. The result showed that the relationship between the coefficient of restitution and damping coefficient affects the nonlinear viscoelastic model of impact force. The stiff impact spring is the essential parameter in this study during the impact force calculation [25].

Khatami et al., (2019) studied the effects of different parameters on the peak impact forces during pounding between adjacent buildings under nine various ground motions. Two adjacent buildings with a single degree of freedom (SDOF) are considered. The nonlinear viscoelastic model has been assumed to be a numerical simulation for colliding bodies to evaluate the impact force during the collision. They discussed two different parameters to verify their influence on the pounding response. The primary parameter is represented by the various ground motions with various PGA and frequency, and secondary parameters, which are natural period, damping ratios, gap size, and coefficients of restitution. For the primary parameters, the result showed that the pounding force does not depend on the PGA, while it relates more to the frequency of ground motions. Moreover, the result showed that the pounding depends on all parameters throughout the analysis where impact force reduced when the damping ratio increased. Also, it showed that the impact force decreased when the gap size increased [26].

2.4.2 Multi Degree of Freedom (SDOF)

Jankowski (2004) studied nonlinear modeling of the earthquake-induced pounding of buildings. Two and three-story of adjacent buildings were chosen. The nonlinear viscoelastic model was simulated as a gap element. Nonlinear time history analysis was carried out. In the study, the left-side building was supposed lighter while the right-side one was assumed heavier. Also, the study fulfilled the different parameters like damping coefficient, gap size, and also mass. The results showed that the gap size mass, stiffness, and damping coefficient significantly affected the more flexible and lighter structure by amplifying responses (displacement). Another hand, the heavier and stiffer structure were affected negligibly [27].

Komodromos, et al., (2007) studied the response of multi-degree freedom isolated buildings concerning the pounding. Three and five-story seismically isolated with different widths of the gap under various ground motions. Two models have the same characteristics (story stiffness, isolation stiffness, masses, damping). A linear viscoelastic model was used to connect the models. The results showed that the floor acceleration and floor deflection decreased when increased the gap size, and it seemed it depends on the properties of the earthquake. The peak inter-story deflection increased with increased impact stiffness until it reached the maximum level and then rest constantly for the greater values of the impact stiffness.
The peak floor accelerations extensively increased with an increase in the impact stiffness value, particularly at the isolation level (base floor). Finally, to optimize both response acceleration and deflection, the gap size, impact stiffness, and flexibility isolation system should select perfect [28].

Mahmoud, et al., (2013) studied earthquake-induced pounding between equal height multi-story buildings considering soil-structure interaction. Two of adjacent with three adjacent buildings have been modeled. A set of ground motions with different PGA from different soil types have been taken in the study. A nonlinear viscoelastic model to evaluate pounding force has been used. Response time history showed the results with peak response, and gap sizes have been considered. The results were obtained from the adjacent buildings with SSI compared to those from adjacent buildings without SSI. The SSI reduced the response of displacement, pounding force, and inelastic shear force while it causes an increase in the response of acceleration at all levels. Furthermore, the SSI reduces the energy response quantities of equal height buildings. In addition, the result showed that the SSI decrease in the peak displacement and impact force. The acceleration response increased for all gap size values respected [29].

López-Almansa, and Kharazian (2014) studied a parametric study of the pounding effect between adjacent Rc buildings with aligned slabs. Three and five-story of adjacent buildings were chosen. The Kelvin-Voight linear gap model connects the adjoining building to calculate pounding force. Nonlinear dynamic analysis with plastic hinges considered was done by Seism-Struct (Seism-Soft 2013). Four different input ground motions from different soil types and different impulsive were selected to apply the adjacent building during pounding. The study was used different configurations for the structure to determine their behavior during pounding. The result showed that the pounding causes to increase outside inter-story drift significantly in the flexible and less stiff buildings. It also enlarges the inside inter-story drift in the floor above the pounding level. It also noticed that the pounding does not affect seriously in the base shear and story shear forces. Furthermore, the pounding leads to increased outside acceleration in both right and left buildings, particularly in the contact level [30].

Zou, et al., (2014) studied Seismic pounding between adjacent buildings of unequal floor height. The study considered two of five adjacent story buildings with unequal floor levels to investigate the inter-floor influence by examining different parameters under the El Centro earthquake. The results were obtained from adjacent buildings with equal floor height compared to those with unequal floor height. The results showed that unequal floor height is less than those with equal height for the main structure. However, it has a significant effect on the substructures.

Consequently, the pounding force obtained from unequal floor height is more severe than equal floor height. The inter-floor response of pounding adjacent buildings associated with the time ratio and gap size is the same as those with equal floor height [31].

Mate, et al., (2015) studied the comparative between pounding response with different contact technical elements. The study considered three adjacent multi-degree freedom buildings and two software programs: MATLAB and SAP2000, to obtain the pounding response and verify them. Nonlinear time history analysis was done with four different ground motions. The results showed: (1) The displacement obtained from six different impact simulations is more or less the same; therefore, the different impact simulation models have very little change in the peak displacement, (2) The shear force from the right exterior building in the direction of an earthquake is a very untraditional low story, and (3) All impact forces from all impact models are the same unless hertz damped and nonlinear viscoelastic models provide small impact force [32].

Changhai, et al., (2015) investigated dimensional analysis of earthquake-induced pounding between adjacent inelastic MDOF buildings to determine several physical similarities. Two of the three-story adjacent buildings under harmonic excitations were selected. The numerical procedure has been performed by MATLAB programming. The several parameters are examined to determine the effect of the story stiffness, story stiffness ratio, mass ratio of adjacent buildings, structural inelastic, and the gap size. The numerical procedure has been performed by MATLAB programming. The results have shown that the stiffness ratio's effect on0 the displacement and velocity of the left building has three different regions: amplified, de-amplified, and unaffected regions, while the right building's responses change with story stiffness ratio where they reduce with increase the story stiffness ratio. Additionally, the results have been discussed that the mass story ratio has a more significant effect on the velocity response than displacement response for both left and right buildings. However, the pounding force has been affected by mass story ratio more than velocity and displacement. Therefore, it increases with increase the story stiffness ratio. The inelastic characteristics ratio has been influenced by the response of displacement and velocity, where the displacement response decreases with an increase in the ratio of the inelastic characteristic; however, the velocity change corresponding to the stiffness regions [33].

Abdel Raheem, et al., (2019) studied the numerical simulation of potential seismic pounding among adjacent buildings in series. Three adjacent buildings with 3, 6, and 12 story buildings with different configurations under nine ground motions are selected. The linear viscoelastic model was connected between adjacent structures. Nonlinear time history is carried out through ETABS. The results were discussed in displacement, acceleration, story shear mean and maximum responses, impact force, and hysteretic behavior. The effect of pounding was studied for the various gap sizes, under nine ground motions, and then compared with the no-pounding state.

The results showed the seriousness of the pounding effects under earthquake excitation associated with the mode shape of the adjacent buildings, the behavior of input ground motions, the location of the building in series adjacent buildings if it is interior or exterior, so either has one or sided contacts.

Furthermore, the results showed that they generate greater shear force and acceleration response at various story levels for the high-rise building, while they decreased in the short one compared to that of the no-pounding state [34].

CHAPTER 3

THEORETICAL BACKGROUND

3.1 General

During an earthquake, the adjacent structures, such as buildings and bridge segments, may collide if the distance between them is insufficient. This phenomenon is called earthquake-induced structural pounding. The adjacent pounding structures may cause local damage at the contact location. Also, it may leads to significant damages or total collapse to the hitting structures during strong ground motions. For the buildings, the primary reason for structural pounding is the difference in fundamental natural periods (Anagnostopoulos 1988; Anagnostopoulos and Spiliopoulos 1992; Maison and Kasai 1990, 1992; Tena-Colunga et al. 1996; Karayannis and Favvata 2005a, b; Jankowski 2005, 2007, 2008; Komodromos 2008; Mahmoud and Jankowski 2009, 2011; Polycarpou and Komodromos 2010; Mahmoud et al. 2012, 2013; Falborski and Jankowski 2013; Sołtysik and Jankowski 2013; Polycarpou et al. 2014).

The difference in masses or stiffness causes the adjacent buildings to vibrate out of phase during an earthquake. It also increases the probability of the structural collision, as in Figure 3.1. Another hand, pounding in the bridge is usually caused by the spatial seismic effect involved in propagating the seismic wave Jankowski et al., 1998, 2000; Kim et al., 2000; Zanardo et al., 2002; Chouw and Hao 2005), as shown in Figure 3.2 [35].

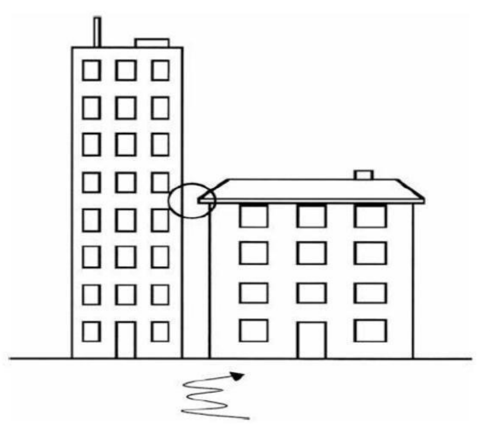

Figure 3.1: Difference in mass or stiffness of pounding between buildings [35].

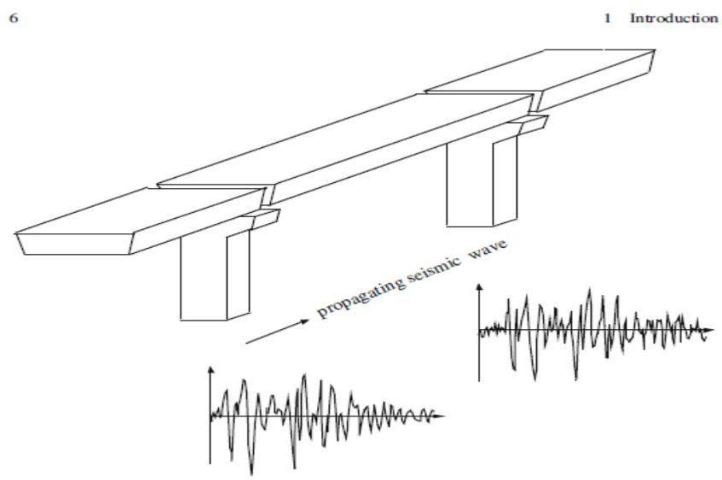

Figure 3.2: Spatial seismic effects related to the propagation of the seismic wave [35].

3.2 Types of Building Pounding

In the last 20 years, building pounding has become a common topic for many researchers worldwide. Unfortunately, other researchers have disagreed with nearly all of these studies, to know more about this phenomenon's behavior requires further knowledge. In this section, the state of adjacent buildings is pounding prepared. Generally, the state-pounding buildings are into two types, as in Figure 3.3[36].

1. Slab-to-slab collision: when the adjacent buildings have the same floor level.
2. Slab-to-column collision: when the adjacent buildings have different floor levels.

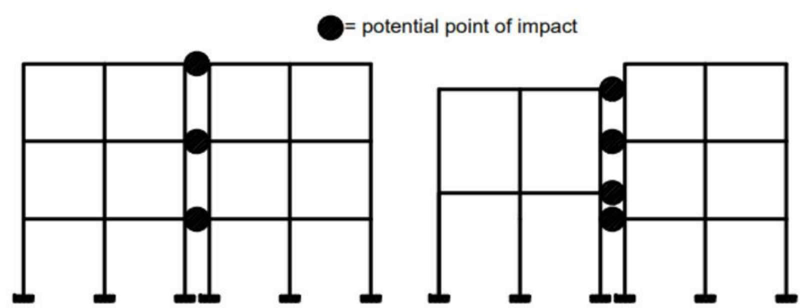

(a) slab to slab collision (b) slab to column collision

Figure 3.3: General scenario for building pounding.

It is possible to assort the pounding buildings into more five groups: a) Pounding of floor-to-floor of adjacent buildings, b) Pounding of floor-to-column of adjacent structures, c) pounding of stiffer to lighter adjacent buildings, d) pounding of taller to shorter adjacent buildings, e) pounding of adjacent torsional buildings, and f) structures are situated in a row with and without similar properties as shown in Figure 3.4. Furthermore, some other studies extend into the sixth type of pounding state, which is the masonry brick pounding building [1-3].

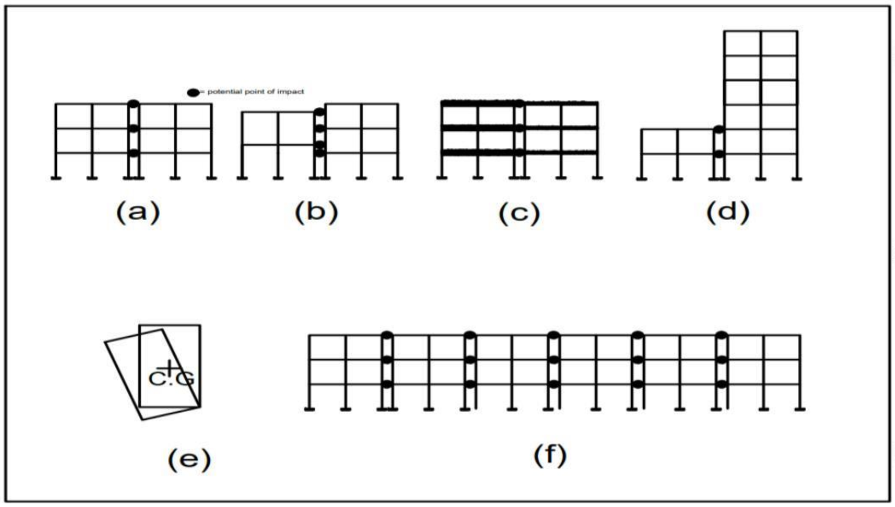

Figure 3.4: Different types for pounding adjacent buildings.

3.3 Impact Structural Model

An accurate structural model needs to be used to estimate the pounding force during an earthquake excitation between adjacent bodies or structures. Two different approaches have been used to simulate the structural pounding.

- Stereo mechanical approach
- Force-based approach

3.3.1 The Stereo Mechanical Model

The stereo-mechanical approach uses the law of the conservation of momentum and energy. The stress and deformation are not considered during impact (Goldsmith-1960). This approach relates directly to the final velocities (v_1' and v_2') and initial velocities (v_1, and v_2) of the bodies to the coefficient restitution (e) as shown in Figure 3.5. See the Equation 3.1, 3.2, & 3.3.

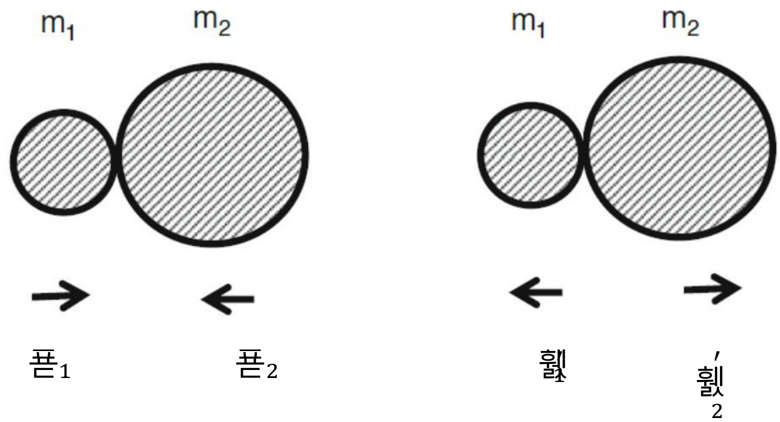

Figure 3.5: Initial and final velocities of contact elements [38].

$$v_1' = v_1 - (1+e)\frac{m_1 v_1 - m_2 v_2}{m_1+m_2} \quad (3.1)$$

$$v_2' = v_2 + (1+e)\frac{m_1 v_1 - m_2 v_2}{m_1+m_2} \quad (3.2)$$

$$e = \frac{v_2' - v_1'}{v_1+v_2} \quad (3.3)$$

The coefficient of restitution can be obtained from experimental by dropping the ball of a particular material with height (h) on the plate plan of the same material and measuring the rebound height (h'), as shown the equation 3.4 (Goldsmith-1960).

$$e = \frac{h'}{\mathrm{h}} \quad (3.4)$$

The value of coefficient restitution is in between 0 to 1, and it depends on being plastic or elastic. When e=0 means the fully-plastic, while e=1 means fully-elastic. It has been found by experimental studies that the value of the coefficient usually ranges from 0.4 to 0.8 (Anagnostopoulos and Spiliopoulos 1992; Zhu et al. 2002; Jankowski 2010). Azevedo and Bento (1996) recommended that e=0.65 for the concrete-to-concrete structure pounding. To obtain the value of the coefficient restitution with different materials can use the following equations 3.5, 3.6 (Goldsmith-1960), as in the Figure 3.6.

$-0.0039v^3 + 0.0440v^2 - 0.01867v + 0.7299$	steel to steel
$-0.0070v^3 + 0.069v^2 - 0.2529v + 0.7929$	concrete to concrete
$-0.0043v^3 + 0.0479v^2 - 0.1971v + 0.7067$	timber to timber
$-0.0040v^3 + 0.0474v^2 - 0.02116v + 0.8141$	ceramic to ceramic

(3.5

$$e = \frac{e_1 E_1 + e_2 E_2}{E_1 + E_2} \quad (3.6)$$

Where e_i and E_i are the coefficients of restitution and modulus of elasticity for material I (i= 1; 2), respectively. The stereo-mechanical approach has no longer used in the structural pounding problems since it ignores the impact period, it does not evaluate the impact force during the collision.

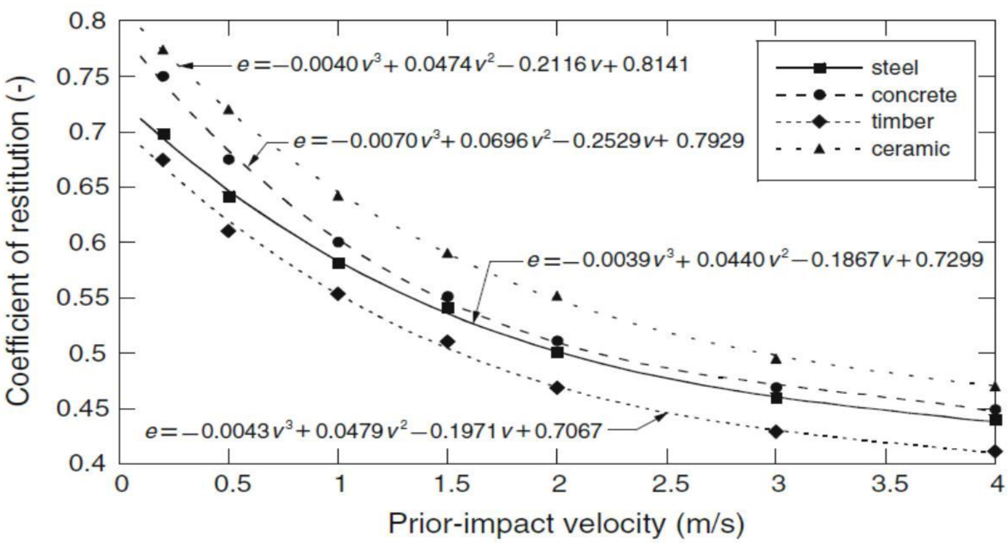

Figure 3.6: Coefficient of restitution with respect to the initial velocity [38].

3.3.2 Force Based Model

The force-based approach can apply to the structural pounding during earthquake excitation and use Instantly the model of pounding force during the collision. One of two impact elements can be simulated for the pounding force between adjacent structures. These two impact elements are: elastic and viscoelastic, as in Figure 3.7. The impact element can be active only when the adjacent structures start to contact.

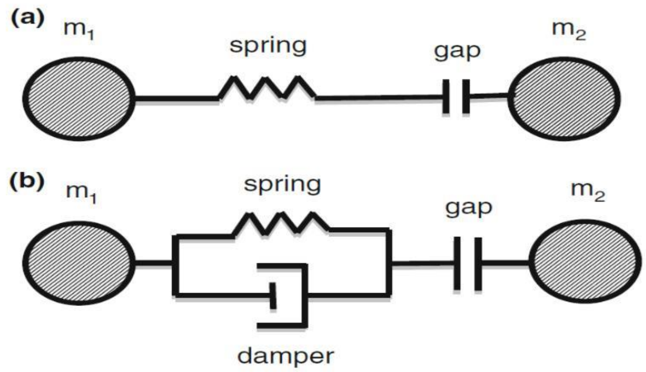

Figure 3.7: Force-based of a) elastic model and b) viscoelastic model [38].

3.3.2.1 Linear Elastic Model

The simplest impact element contains the linear elastic spring (Maison and Kasai 1990, 1992). The pounding force can be described according to equation 3.7.

$$F = \begin{cases} k(u_1 - u_2 - d), & (u_1 - u_2 - d) > 0 \\ 0, & (u_1 - u_2 - d) \leq 0 \end{cases} \tag{3.7}$$

Where u_1 and u_2 are displacement of the colliding bodies, k is the spring stiffness (it is equal to the stiffness of the colliding element at the contact location), *d* is the inertial gap separation. The only negative side of the linear elastic model is that it ignores the energy dissipation during impact (Jankowski-2015).

3.3.2.2 Linear Viscoelastic Model

The linear viscoelastic model (Kelvin-Voigt model) solved the drawback of the linear elastic model where it consists of the spring and damper (Wolf and Skrikerud 1980; Anagnostopoulos1988, 1995, 1996). The pounding force can be expressed in equation 3.8.

$$F = \begin{cases} k(u_1 - u_2 - d) + c(\dot{u}_1 + \dot{u}_2), & (u_1 - u_2 - d) > 0 \\ 0, & (u_1 - u_2 - d) \leq 0 \end{cases} \tag{3.8}$$

Where $\dot{u}_1$, $\dot{u}_2$ are relative velocities of impact bodies, c is the element's damping, which can be solved on the equation 3.9 & 3.10 (Anagnostopoulos-1988, 2004):

$$c = 2\xi\sqrt{k\frac{m_1 m_2}{m_1+m_2}} \tag{3.9}$$

$$\xi = -\frac{\ln e}{\sqrt{\pi^2+(\ln e)^2}} \tag{3.10}$$

Where m_1 and m_2 are mass of the colliding bodies, and ξ is the damping coefficient. The previous equation has no longer been used, so the new question has been proposed by (Mahmoud & Jankowski-2011) as below described equation 3.11.

$$\xi = \frac{1-e^2}{e(e(\pi-2)+2)} \tag{3.11}$$

3.3.2.3 Hertz Nonlinear Elastic Model

Hertz's nonlinear elastic model obeyed the law of the hertz contact (1882). It has been used in several studies (Jing and Young1991). The pounding force can be expressed by equation 3.12.

$$F = \begin{cases} \beta(y_1 - y_2 - g)^{3/2}, & (y_1 - y_2 - g) > 0 \\ 0, & (y_1 - y_2 - g) \le 0 \end{cases} \tag{3.12}$$

3.3.2.4 Nonlinear Viscoelastic Model

The negative side of the nonlinear hertz model is also solved in the nonlinear viscoelastic model (Jankowski-2009,2010 and Mahmoud-2012, 2013). The pounding force can be expressed by equation 3.13.

$$F = \begin{cases} \beta(y_1 - y_2 - g)^{3/2} + c(\dot{y}_1 - \dot{y}_2) & (y_1 - y_2 - g) > 0 \\ \beta(y_1 - y_2 - g)^{3/2}, & (y_1 - y_2 - g) \le 0 \end{cases} \tag{3.13}$$

The element's damping can be calculated by the formula 3.14(Jankowski-2005b), while the damping ratio is calculated from the equation 3.15 (Jankowski-2006b) [38].

$$C = 2\xi\sqrt{\beta\sqrt{(y_1 - y_2 - g)}\frac{m_1 m_2}{m_1+m_2}} \tag{3.14}$$

$$\xi = \frac{9\sqrt{5}}{2}\,\frac{1+e^2}{e(e(9\pi-16)+16)} \tag{3.15}$$

3.4 Infill Wall Modeling

Infill wall is considered non-bearing structural members; it has an impact to the structural masses and rigidities. It is not deemed to be structural members. It is placed inside of frame (beam and columns) boundaries [37]. According to the Turkish seismic code (TSC-2007), the infill walls are allowed only as vertical uniform loads on the beams and floors on the design of the RC structures. However, the infill wall in framed structures can affect the dynamic behaviors of the structures. The dynamic behavior of the structure can be stiffness, strength, and ductility [38].

To model of infill walls, there are two methods for infill wall modeling. These are macro-modeling and micro-modeling. The macro-modeling method relates to the equivalent strut method, where the micro-modeling refers to the finite element method. Several studies have been used by the equivalent-strut method for both steel and RC frame. To model the infill wall through the equivalent strut method, the width of the strut diagonal is necessary. To calculate the diagonal strut width can be used in many ways. In this study, diagonal strut width can obtain from the FEMA 356 see equations 3.16-17 [37].

$$\lambda_h = \sqrt[4]{\frac{E_{me} t_{inf} \sin(2\theta)}{4 E_{fe} I_{col} h_{inf}}} \tag{3.16}$$

$$a = 0.175 d (\lambda_h h_{col})^{-0.4} \tag{3.17}$$

Where the E_{me} is the modulus of elasticity of infill wall, E_{fe} is the modulus elasticity of frame, I_{col} is the moment inertia of column, h_{inf} is the height of the infill wall, θ is the slope angle of the strut diagonal, λ_h is the reduction factor for diagonal strut width, a is the width of strut diagonal.

The parameters of h_{inf}, l_{inf}, d, E_{me}, and θ can be obtained from the below formula 3.18-3.22[39].

$$h_{inf} = H_{col} - h_{beam} \tag{3.18}$$

$$l_{inf} = L_{beam} - h_{col} \tag{3.19}$$

$$퐝=\sqrt{퐿^{2}+퐻^{2}} \tag{3.20}$$

$$퐸 \;=550 \qquad \text{(FEMA-356)} \tag{3.21}$$

$$\theta=푡푎푛^{-1}\left(\frac{퐻푖푛푓}{퐿푖푛푓}\right) \tag{3.22}$$

Where the $h_{퐛퐦}$ is the beam section height, $h_{퐜표퐥}$ is the column section heigh, $퐿_{퐛퐦}$ is the length of the beam, and is the compressive strength of the infill wall. See the Figure 3.8.

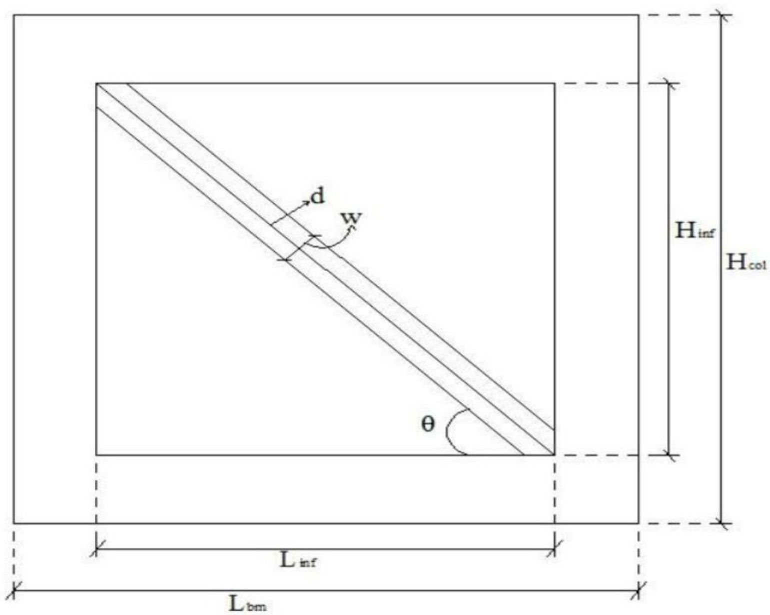

Figure 3.8: The strut diagonal of infill wall design.

3.5 Review of Analysis Method

In this study, the pounding adjacent buildings with different configurations under the influence of ground motions have been considered. Two adjacent buildings having bare frames and infill walls have been taken into account to evaluate the pounding effectiveness of adjacent buildings. Nonlinear time history analysis has been taken to evaluate the model results. The seismic parameters such as story displacement, drift ratio, pounding force, and acceleration were compared.

3.5.1 General

Time history analysis is the dynamic method that taken place step by step analysis to evaluate the response of a structure for each step of the particular lateral load that may vary with time. It is used to define the seismic response of structure when the dynamic load is subjected to the structure which earthquake represented (Wilkinson and Hiley, 2006), as Figure 3.9. Time history analysis can be given a linear or nonlinear dynamic response structure under various loading times. The dynamic equilibrium equation can be solved by a model or direct integration method.

m퓮(퓭)+c퓮 (3.23)

m, c, and k are mass coefficient, damping coefficients, stiffness matrices, and F(t) is external load vector, while the 퓮(퓭), 퓮(퓭), and 퓮(t) are acceleration, velocity, and displacement vectors as shown in equation 3.23.

3.5.2 Nonlinear Time History Analysis

Nonlinear direct integration time history analysis has been considered throughout the study. Five different ground motions in the near-fault region have been subjected to the building models in the analysis.

The geometry nonlinearity included the P-Delta effect during direct integration, while plastic hinges are assigned for both ends of beams and columns. The 0.5 and 0.25 are selected for Newmark-direct integration coefficients of α and β, respectively. The damping ratio was taken to be 5%.

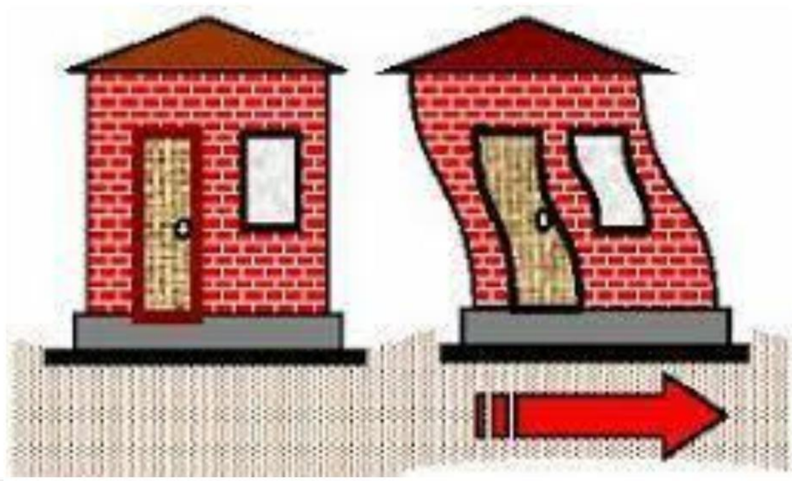

Figure 3.9: Effects on a building under earthquake ground motion [40].

P-Delta effect is a type of geometric nonlinearity which is related to the compatibility relationship of structural members. In general, the p-delta effect can be classified into two categories: Large P-Delta and small P-Delta effects, as shown in Figures 3.10, and 3.11. The large P-Delta effect is related to the displacement of the member at the ends. In contrast, the small P-Delta effect is related to the local deformation relative to the element chord between end nodes.

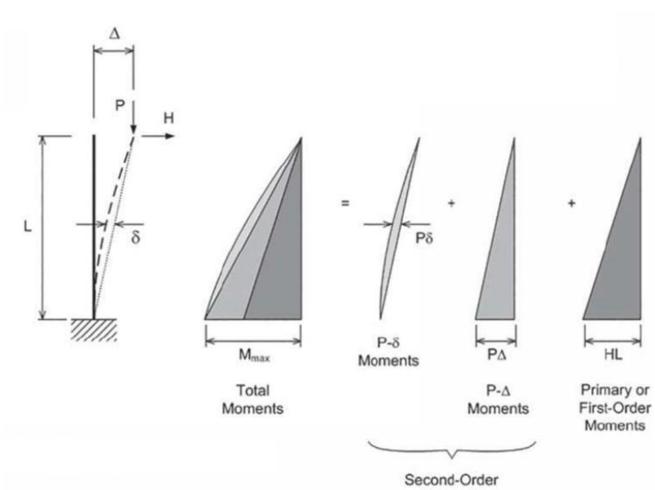

Figure 3.10: P-Delta effect (P- 훪 and P- 훽)in column [41].

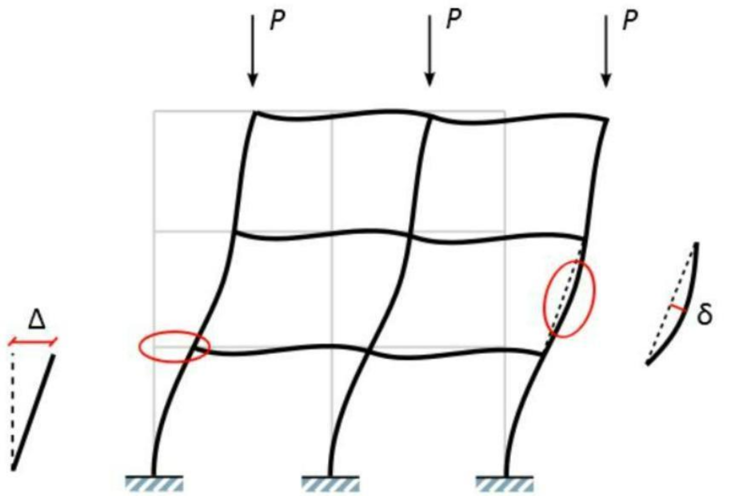

Figure 3.11: Global and local second-order effect in building [42].

Plastic hinge has defined the deformation that occurred at the beam or column, sections where plastic bending takes place. In nonlinear analysis, plastic hinges are very important to check the performance and failure of the structure under seismic loading, see Figure 3.12.

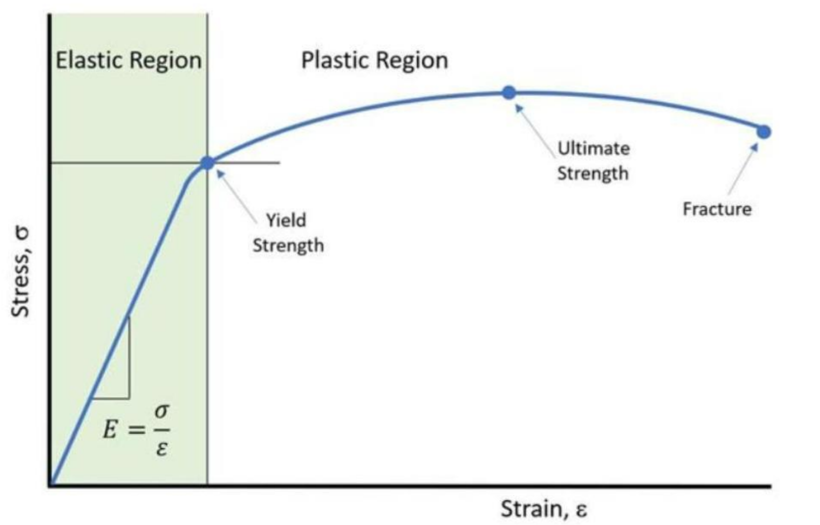

Figure 3.12: Elastic and plastic, region deformation (SIMSOLID) [44].

CHAPTER 4

NUMERICAL MODELING OF POUNDING

4.1 Introduction

This chapter will present the pounding behavior of adjacent buildings being bare-frame and adjacent buildings with infill walls under seismic excitation. Hertz Non-linear Elastic Model with 0.5mm gap separation is considered to model pounding force. Nonlinear time history analysis was carried out using the SAP2000 program. The equivalent static method has been used for design structures. Five horizontal ground motions with various PGA and M_w have been taken. The ground motions have been scaled and matched with the target response spectrum through Seismo-Macht software.

4.2 Description of Buildings

Two different 2D of RC adjacent buildings with different configurations have been studied, as shown in Figure 4.1. The adjacent buildings of 9 and 6 stories are assumed. Both buildings have the same floor level and same bays: 3m and 5m, respectively. The column and beam dimensions are 0.60mx0.60m and 0.60mx0.30m for the nine-story building, while the column and beam dimensions are 0.50mx0.50m and 0.50mx0.30m for a six-story building. The partition infill wall thickness is 0.178m. The dimensions are summarized in Table 4.1.

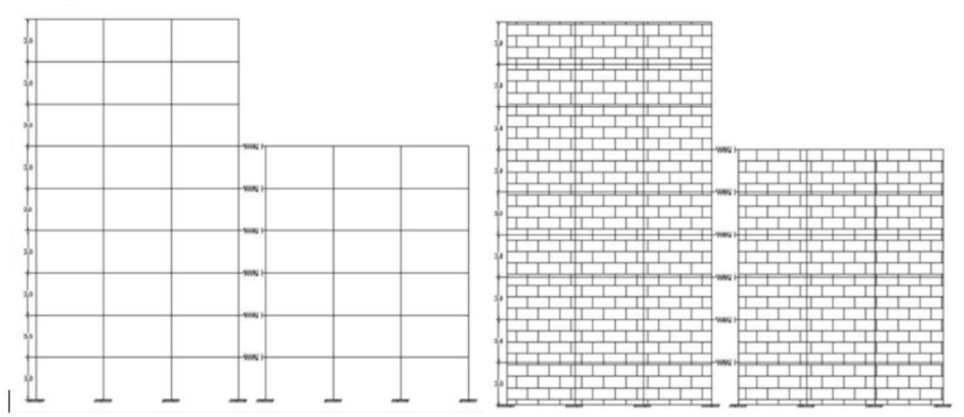

(a) (b)

Figure 4.1: Adjacent buildings with different scenarios for a) bare frame and b) infill wall.

Table 4.1: Specification of building dimensions**.**

Frame type	Column(mm)	Beam(mm)	Infill wall (mm)
9-story	600x600	600x300	178x178x381
6-story	500x500	500x300	178x178x381

Moreover, the infill wall thickness (t) is 178mm for both buildings. Strut width (w) is 631mm and for the nine-story building, while 604mm for the six-story building.

4.2.1 Material Properties

The construction materials used for the buildings were verity. These materials are concrete, rebar, and masonry. These materials have been selected from European-code (EU) standard. The properties of each of these materials are described in below Table 4.2.

Table 4.2: Specification of material properties.

Material name	**Grade**
Concrete	**C25/30**
weight per unit volume(kN/m^3)	25
Modulus of elasticity (GPa)	31
Poisson ratio	0.2
Rebar	**S420**
Modulus of elasticity (GPa)	200
The yield of strength (MPa)	420
Ultimate yield of strength (MPa)	500
Masonry	**C90**
Weight per unit volume (kN/m^3)	16.5
Modulus of Elasticity (GPa)	7.15
Poisson ratio	0.2

4.2.2 Design Loads

The building was designed for people to live in (Residential) with a dead load of 15kN/m, superimposed dead load from walls of 7.3kN/m, and live load of 10kN/m. However, according to TSC2018, the equivalent lateral load parameters are presented in Table 4.3.

Table 4.3: Equivalent force parameters for design.

parameter' Name	Evaluation
Site class	ZB
occupancy importance, I	1
response modification factor, R	8
map spectral acceleration coefficient, S1	0.16
short spectral acceleration coefficient, Ss	0.522
Long-period	6
Peak ground acceleration, PGA	0.85

4.2.3 Load Combination

Load combination is the combination of loads that are more than one type subject to the structure. Building code always describes a different load combination with factors for each load type to ensure structural safety. It is combined by allowing the standard of TS500-2000(R2018). The list of Load combinations is shown below:

- ✓ 1.4G +1.6 Q
- ✓ G + Q
- ✓ G +Q +EX
- ✓ G + Q -EX

Where G is dead load, Q is live load, and EX is earthquake load.

4.2.4 Reinforced Details of Frame Sections

The minimum requirement reinforcement details of the frame sections can be designed through SAP 2000. The frame sections (column & beam) imported into the SAP2000 program applied both the gravity and lateral load to the structure verified frame sections to make sure either frame section fails. The Largest longitudinal and shear rebar areas were selected. To express more details related to the RC details are in Figure 4.2 and Table 4.4.

Table 4.4: Beam and column reinforcement details.

9-story	**R.C details**
Column(600x600mm)	Long=8Ø25mm shear=3Ø10 @150mm b/w
Beam(600x300mm)	Top=3Ø18 Bottom=2Ø18
6-story	**R.C details**
Column(500x500mm)	Long=8Ø20mm shear=3Ø10 @150mm b/w
Beam(500x300mm)	Top=4Ø16mm Bottom=2Ø16mm

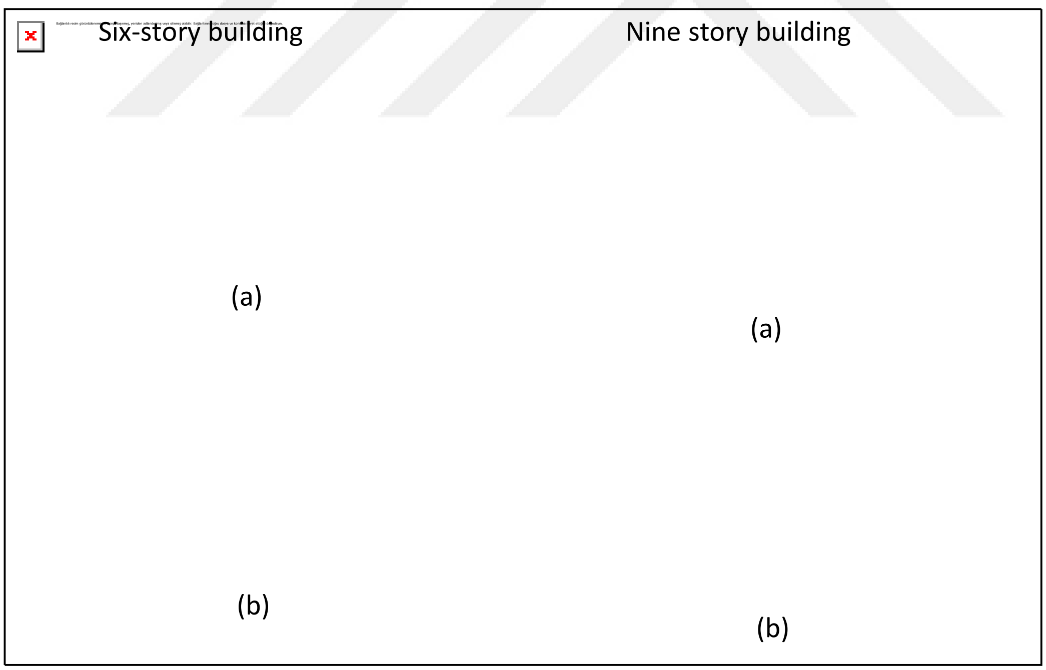

Figure 4.2: Reinforcement details for both buildings a) column, and b) beam.

4.2.5 Gap Element Modeling

In order to obtain the pounding force between adjacent buildings, those that have a small separation distance during earthquake excitation, the gap element should be placed between adjacent buildings. The gap element has two joints, L and R, and connects the left and right buildings at each floor level.

The gap element becomes active only when the gap became zero. Pounding adjacent buildings is simulated using the nonlinear elastic model (hertz model). The force goes through from one structure to another by means only when the nonlinear spring touch occurs. The force-deformation relationship of the gap element is given by equation 3.12. Nonlinear spring model is consideration as 1,130,000kN/m$^{1.5}$ for concrete-to-concrete impact element as Jankowski (2005) suggested.

4.2.6 Input Ground Motion

In this study, five different horizontal ground motions are selected to use. These ground motions are obtained from the PEER ground motion database as a pre-scaled form and matched with the target design response spectrum using Seismo-Macht as Figure 4.3. All ground motions range between 0.20g to 0.25g and 6.0 to 7.2 of peak ground acceleration and magnitude, as shown in Table 4.5.

Table 4.5: Specific characteristics of the different ground motions.

No	Earthquake's Name	Year	Station	Mw	PGA(g)
	Imperial Valley-02	1940	El Centro Array #9	6.95	0.22
2	Kobe_ Japan	1995	Amagasaki	6.9	0.27g
3	El Mayor-Cucapah_ Mexico	2010	CERRO PRIETO GEOTHERMAL	7.2	0.2
4	Darfield_ New Zealand	2010	DSLC	7	0.21
5	El Mayor-Cucapah_ Mexico	2010	Westside Elementary School	7.2	0.24

Where PGA is peak ground acceleration and mw is the magnitude of the earthquake.

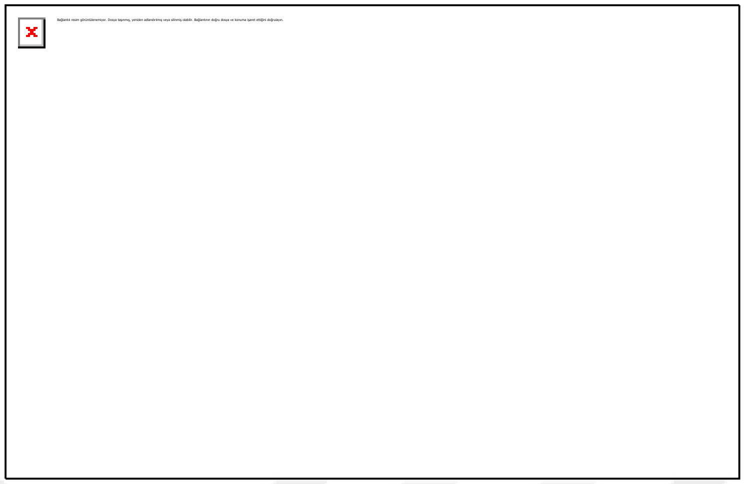

Figure 4.3: Mean of ground motions to target spectrum (PEER).

4.2.6.1 Scaling of Ground Motion Recoded Data

In this section, the scaling ground motion acceleration has been done. The significance of scaling is getting close appropriate to the target response spectrum, which can respond to the structure's response assessment. The comparison between the target response spectrum and the response spectrum of scaled ground motions is in Figure 4.4. Further information on the several different sides of the scaling procedures is available in the past study (Miranda 1993, Vidic 1994; Kalkan & Chopra 2011). Finally, the Seismo-Macht software program has been used to obtain the real and scaled ground motion acceleration.

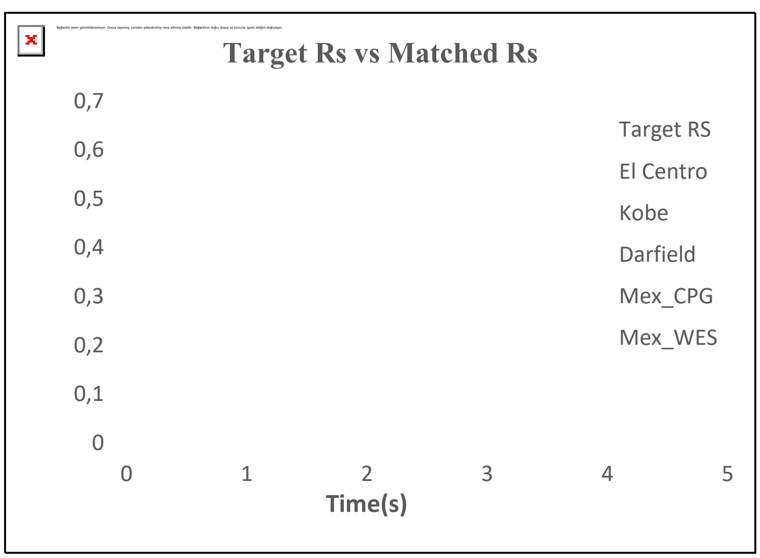

Figure 4.4: Comparison between matched RS with target RS.

4.3 Modeling in SAP2000

To implement the modeling and analysis of the 2D-RC frame of adjacent buildings, SAP2000 has been utilized for modeling the structures. For modeling adjacent buildings with and without infill walls, the SAP2000 software program has been used to implement. The complete procedures for the adjacent building with bare-frame and infill walls have been clarified step by step by using SAP000.

4.3.1 Bare Frame's Adjacent Buildings Modeling

First, the adjacent building with bare frame only has been completed modeling in side sap2000. The procedures have been described step to step:

1. The first step for modeling adjacent buildings in SAP200 is to define a material property by determining the specific code. In this study, the EU standard was selected has been utilized to carry out this study as shown in Figure 4.5.

(a) (b)

Figure 4.5: Determining the material properties a) for concrete, and b) for rebar.

2. The second step to model is to define the frame section properties. Beam and column are represented as a frame section. Both columns and beams sections for the adjacent buildings are shown in figure 4.6.

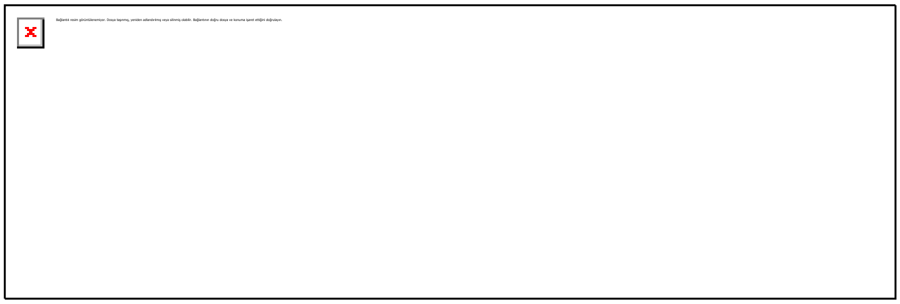

(a) (b)

(b) (d)

Figure 4.6: Frame section (beam and column) defining a) column for left building, b) beam for left building c) column for the right building, and d) beam for the right building.

3. The third step is to model the adjacent buildings to define the load pattern. Both the gravity and lateral loads are used to design the member of the structure. Dead and live loads are representative of the gravity load, where the equivalent static force is representative to be lateral load, as in Figure 4.7.

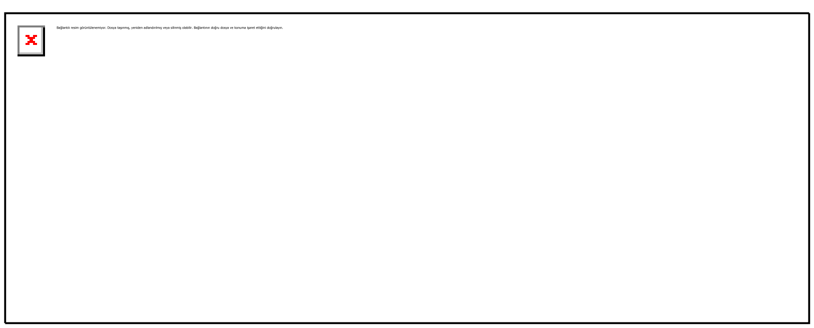

Figure 4.7: Defining load pattern.

4. After the load pattern, the load case was defined. The load case shows all loads from the load pattern. The gravity load was added in load case by nonlinear case as shown in below Figure 4.8.

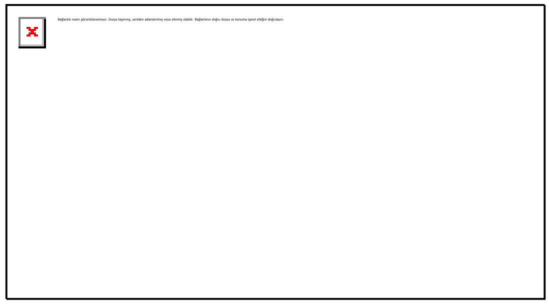

(a)

(b)

Figure 4.8: The load case defining.

5. The mass source was defined by using TS500-2000(R2018). The TSC suggested 100% of the dead load and 30% of the live load as shown in the below Figure 4.9.

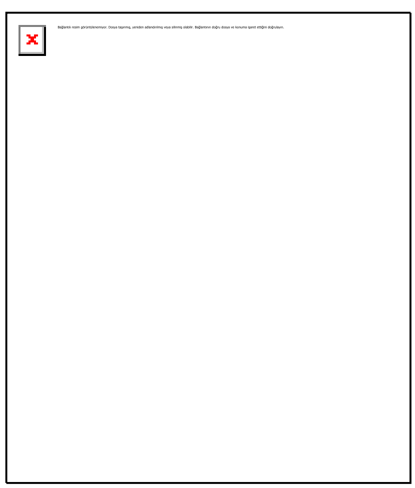

Figure 4.9: Mass source defined.

4.3.2 Adjacent Buildings with Infill Wall Modeling

A masonry infill wall was placed in the frame (between beam and column) for each building. To model masonry infill wall according to the ASCE41-06 was modeled as equivalent diagonal strut (w). Cross diagonal strut infill wall was modeled with different strut widths for each left and right buildings. The strut width of 631mm and 604mm for left and right of adjacent buildings, respectively. The thickness of the infill wall was 178mm. To model the strut diagonal inside SAP2000, the below steps shall be following.

- Define masonry infill properties (Figure 4.10).

Figure 4.10: Infill wall material (masonry) property defined.

- Define the diagonal strut section with t=178mm for both buildings, and width of 631mm, and 604mm for left building and right buildings, respectively (Figure 4.11).

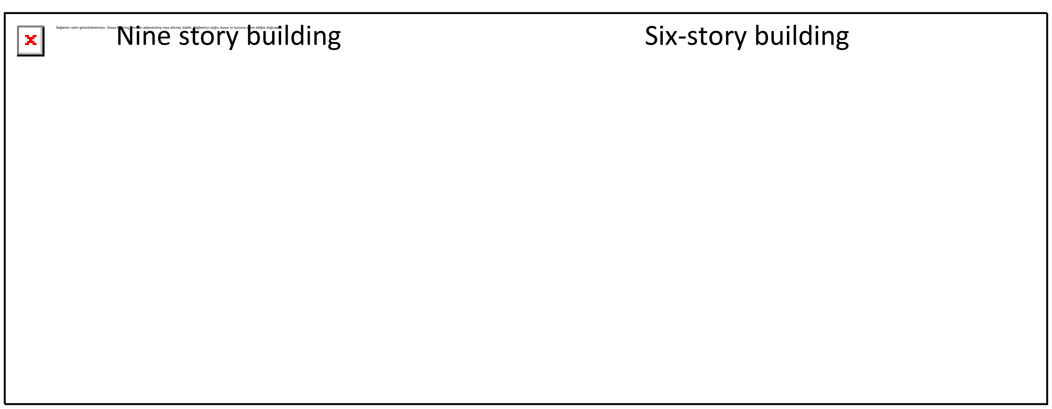

Figure 4.11: Defined of equivalent strut diagonal section.

- Draw the braces by x-shape (Figure 4.12)

Figure 4.12: Infill wall modeling inside sap2000.

- Finally, assign the strut diagonal member to carry compressive only (Figure 4.13) and assign the member releases and partial fixity with zero Moment3-3 as in Figure 4.14.

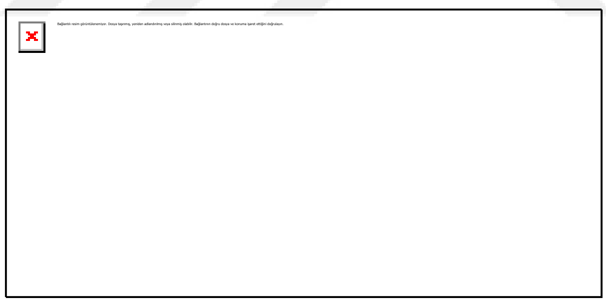

Figure 4.13: Assigned infill wall (strut diagonal) for compression only.

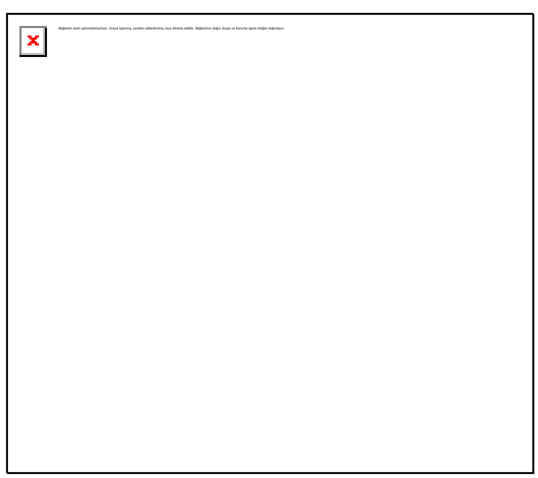

Figure 4.14: Assigned infill wall (strut diagonal) with zero moment-33.

4.3.3 Time History Analysis Modeling Inside SAP2000

First, the time history function was defined in the SAP2000 as shown in Figure 4.15. Ground motion data was inserted in the SAP2000 as in the Figure.

Figure 4.15: Time history analysis function defined.

In the next step, the gravity load was defined by a combined 100% of dead load and 30% of live load (DL+0.30LL). The gravity load is considered as nonlinear static load by selecting geometry nonlinearity to determine the P-Delta effect as Figure 4.16.

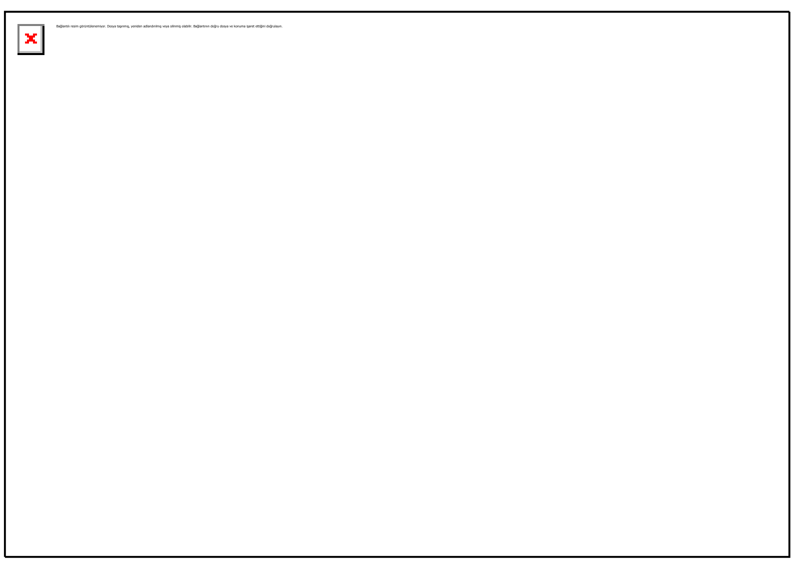

Figure 4.16: Gravity nonlinear static load defining.

Finally, nonlinear time history analysis was defined as shown in Figure 4.17. As described in the analysis direct integration was taken as a solution type, while P-Delta was selected in geometric nonlinearity parameters. It continued from the end of the previous nonlinear static case.

Figure4.17: Parameter of time history analysis detail.

4.3.4 Plastic Hinge Properties

The relative distance of the plastic hinge for both beams and columns was assigned as 0 and 1 at the start and end as mentioned in FEMA 356[46]. The auto hinge type for both beam and column is selected from the table in ASCE41-13.

The degree of freedom of M3 and P-M2-M3 have been selected for beams and columns, respectively. The plastic hinge is important for defining the material nonlinearity of the structure. However, the plastic formation is shown in the below Figure 4.18-19.

Figure 4.18: Beam assigned -Hinge.

Figure 4.19: Column assigned -Hing.

CHAPTER 5

ANALYSIS, RESULTS, AND DISCUSSIONS

5.1 General

Non-linear time history analysis has been performed in two different adjacent buildings inside SAP2000 v.21. Five horizontal ground motions with various PGA and M_w are utilized. Adjacent buildings of nine and six-story with a bare frame and with infill walls are considered during this study:

1. The results of adjacent buildings with a bare frame (BF) are described in the form of graphs and tables.
2. Adjacent buildings with infill walls (IW) are mentioned.
3. Both cases have been compared by using tables and graphs.

5.2 Analysis Results

Nonlinear time history analysis has been carried out to obtain the response of pounding adjacent buildings. The pounding influence on the different cases of adjacent buildings is testified by using time history nonlinear analysis. The results obtained from both cases are compared to assess which case has more effectiveness**.**

5.2.1 Bare Frame's Adjacent Buildings

In this section, adjacent buildings of nine and six-story with the bare frame were subjected to lateral forces of five horizontal ground motions are representative. Both LB and RB have been discussed in the form of story displacement, story drift ratio, pounding forces, and acceleration at pounding level.

5.2.1.1 Story Displacement

The responses of the structure in the longitudinal direction are obtained. Figure 5.1 shows the maximum story displacement building in the longitudinal direction. The highest displacement of both buildings (LB and RB) has occurred at the roof level.

The maximum response story displacement of the adjacent buildings (LB and RB) for each ground motion is shown below Figure 5.1. For the left building (LB), the highest roof displacement is 46mm under the El Centro earthquake, and the lowest roof displacement is 37mm under Kobe, and Mexico_CPG earthquakes, respectively. The El Centro is 1.26 times greater than Kobe and Mexico_CPG earthquakes. For the right-building (RB), the highest roof displacement is 41mm, while the lowest roof displacement is 27mm under El Centro and Mexico_CPG earthquakes, respectively. El Centro is 1.51 times greater than the Mexico_CPG earthquake.

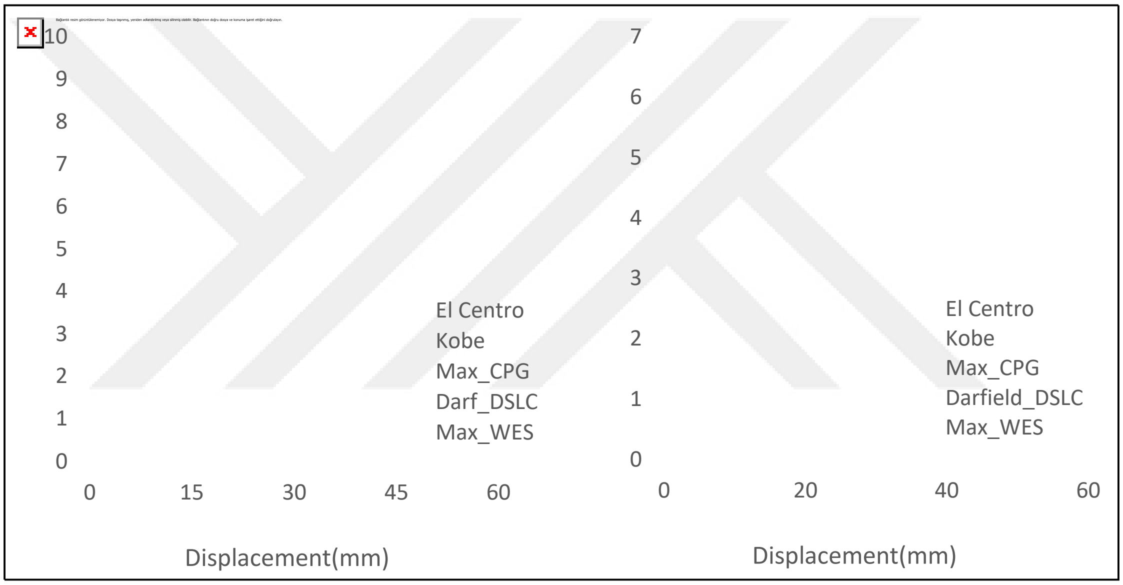

(a) **(b)**

Figure 5.1: Maximum story displacements of a) LB and b) RB.

5.2.1.2 Story Drift Ratio

Figure 5.2 shows the maximum story drift ratio for each floor level of buildings for the different horizontal ground motions. The highest drift ratio occurs at the middle floor level of the buildings. For the left-building (LB), the highest story drift ratio is 0.259% under the El Centro earthquake, and the smallest drift ratio is 0.206% under the Mexico_WES earthquake. Thus, the highest drift ratio obtained from El Centro is 1.3 times greater than the Mexico_WES earthquake. For the right-building (RB), the highest story drift ratio is 0.333% under the El Centro earthquake, and the smallest story drift ratio is 0.23% under Mexico_CPG earthquakes. Thus, the El Centro is 1.4 times more than the Mexico_CPG earthquake.

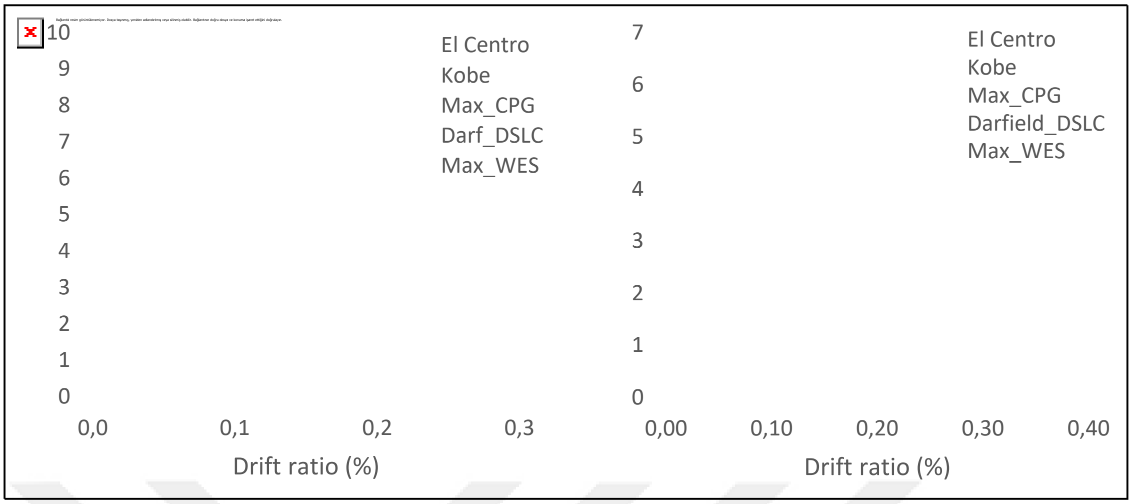

(a) (b)

Figure 5.2: Maximum story drift ratio of a) LB and b) RB.

5.2.1.3 Pounding Force

Table 5.1 shows the pounding force produced in the link element at each floor level (from 1-to-6). The greatest-pounding force was noticed only at the highest pounding level and at the other floor level (fifth), while the smallest one occurs at the lowest floor level. The largest-pounding force is 576kN, and the smallest one is 322kN under El Centro and Max_CPG earthquakes, respectively. It has been reduced by 44%.

Table 5.1: Pounding force variation with height for bare frame adjacent buildings.

LINK	El Centro(kN)	Kobe(kN)	Mex_CPG(kN)	Darfield(kN)	Mex_WES(kN)
1	48	0	0	56	42
2	179	60	106	174	160
3	215	169	156	258	197
4	292	284	305	355	253
5	412	378	322	397	287
6	576	405	279	324	332

Figure 5.3 shows the pounding forces under various ground motions. From the graph, the pounding forces have similar shapes under all ground motion unless the Darfield and Mexico_CPG were the greatest pounding force noticed at the fifth-floor level.

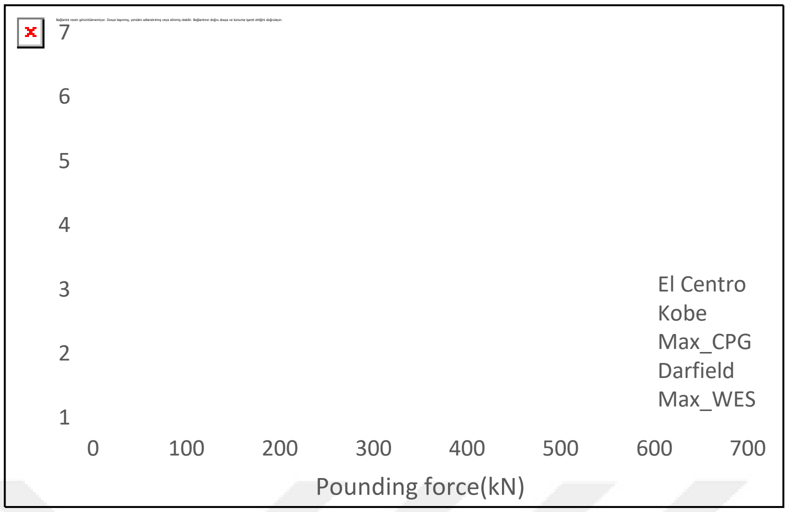

Figure 5.3: Maximum pounding force for each ground motion.

5.2.2 Adjacent Buildings with Infill Wall

In this section, the adjacent buildings of nine and six stories with having infill walls were subjected to lateral forces of five horizontal ground motions are representative. The results of both LB and RB have been discussed in the form of story displacement, story drift ratio, pounding forces, and acceleration at pounding level.

5.2.2.1 Story Displacement

Figure 5.4 shows the maximum response displacement at each floor level for adjacent buildings (LB & RB). The highest displacement occurs at the roof level. For the LB, the highest displacement is 22mm under the El Centro earthquake, and the smallest displacement is 19mm under the Mexico_CPG earthquake. Thus, it has been reduced by 13.1%. However, the displacements were given by the other four ground motions that occur between El Centro and Mexico_CPG earthquakes.

For the RB, the highest displacement is 15mm under the Kobe earthquake, and the smallest displacement is 13mm under the Mexico_CPG earthquake. Therefore, it has been reduced by 12.9%.

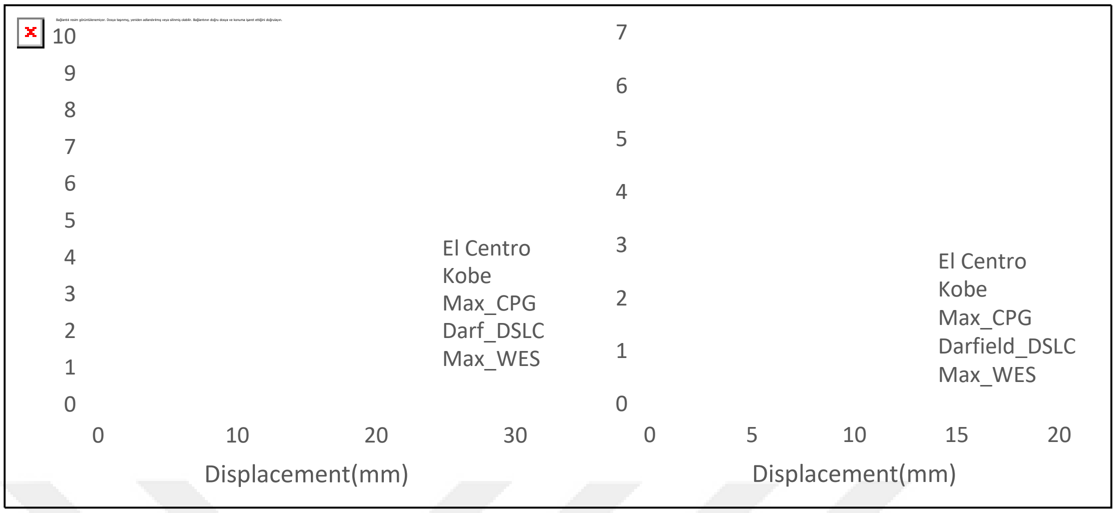

(a) (b)

Figure 5.4: Maximum story displacements of a) LB and b) RB.

5.2.2.2 Story Drift Ratio

Figure 5.5 shows the maximum story drift ratio for each floor level of buildings for the different horizontal ground motions. The highest drift ratio occurs at the middle floor level of the buildings. For the left-building (LB), the highest story drift ratio is 0.112% under the El Centro earthquake, and the smallest drift ratio is 0.098% under the Mexico_CPG earthquake. It has been reduced by 13.07%.

For the right-building (RB), the largest story drift ratio is 0.108% under the Kobe earthquake, and the smallest story drift ratio is 0.087% under Mexico_WES earthquakes. Thus, it has been reduced by 18.9%.

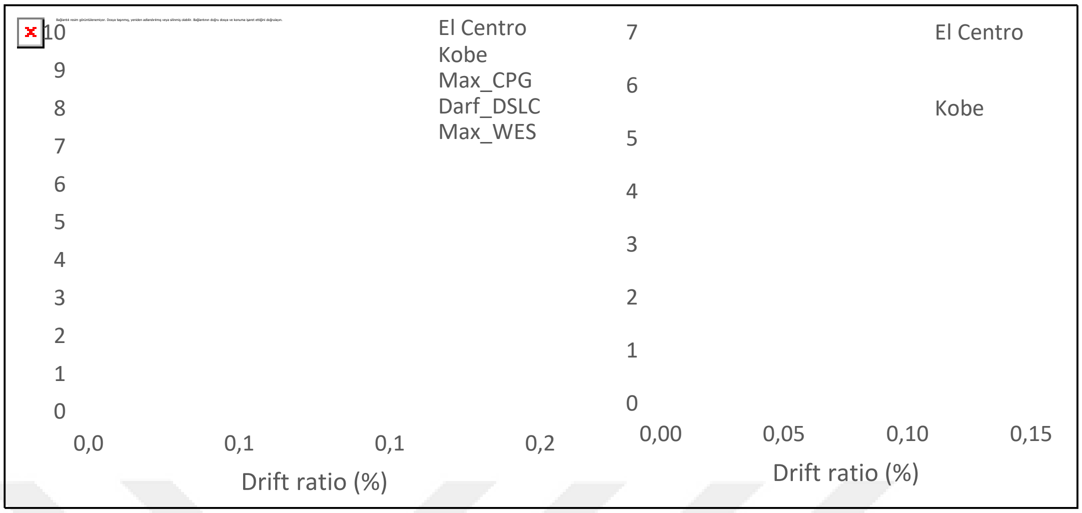

(a) (b)

Figure 5.5: Maximum story drift ratio of a) LB and b) RB.

5.2.2.3 Pounding Force

Table 5.2 shows the pounding force generated in the link element at each floor level (from 1-to-6). Generally, the greatest-pounding force occurs at the pounding level, while the smallest one is taken place at the lowest floor level. The highest pounding force is 879 kN under the El Centro earthquake, and the smallest one is 508kN under the Mexico_CPG earthquake. It has been reduced by 42.2%. Figure 5.6 shows the pounding forces for the adjacent building when different ground motions are applied.

Table 5.2: Pounding force variation with height for adjacent buildings with infill wall.

LINK	El Centro(kN)	Kobe(kN)	Mex_CPG(kN)	Darfield(kN)	Mex_WES(kN)
1	81	82	130	111	71
2	333	268	345	293	228
3	354	316	414	412	367
4	536	417	411	562	363
5	544	469	472	611	578
6	879	669	508	761	783

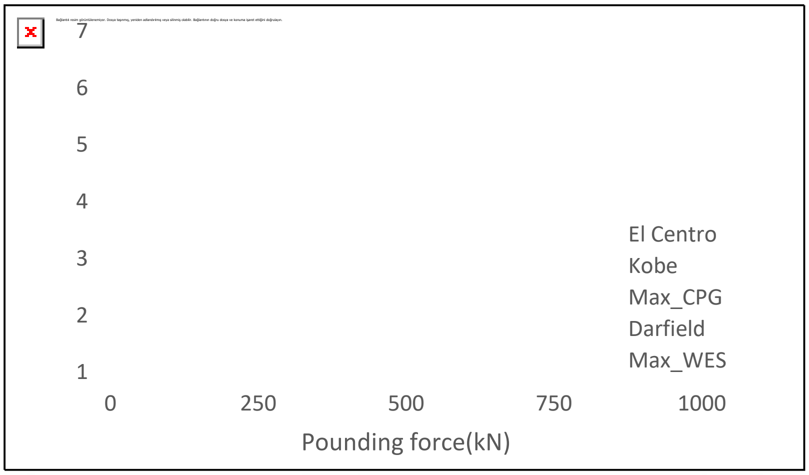

Figure 5.6: Maximum pounding force for each ground motion.

5.2.3 Compression Between Adjacent Buildings of Bare Frame and Infill Wall

The main focus of this study is to determine the effectiveness of the pounding on the adjacent buildings during earthquake excitation. The results from bare frame's adjacent building and adjacent building with infill wall during an earthquake excitation have been compared to determine their effectiveness. The El Centro, Kobe, and Mex_WES earthquakes have been selected to analyze pounding adjacent buildings. The results have been shown the story displacement, story drift ratio, pounding force, acceleration history, and pounding force history at the pounding level.

5.2.3.1 Story Displacement

Figure 5.7 mentioned the difference between maximum displacement at each floor level for left adjacent buildings (LB) with bare frame and infill wall cases. The highest displacement for both cases occurs at the roof level of the building. The highest roof displacement for the bare frame's case is 46mm, 37mm38mm under El Centro, Kobe, and Mex_WES earthquakes, respectively, while for infill wall case is 22mm, 21mm, and 20mm under El Centro, Kobe, and Mex_WES earthquakes respectively. Thus, it has been reduced by 52.7%, 43.1%, and 49% under El Centro, Kobe, and Mex_WES earthquakes.

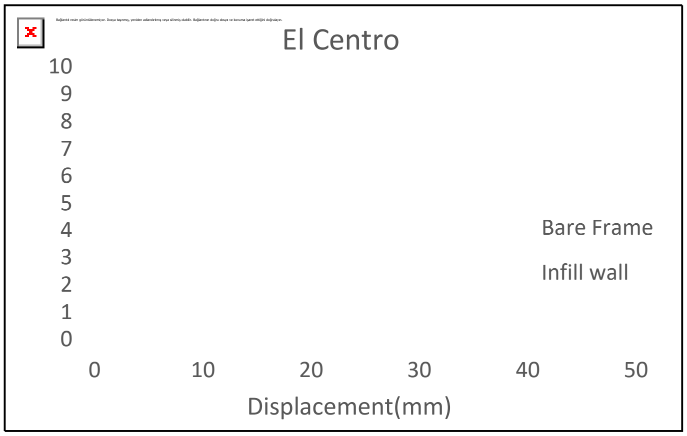

(a)

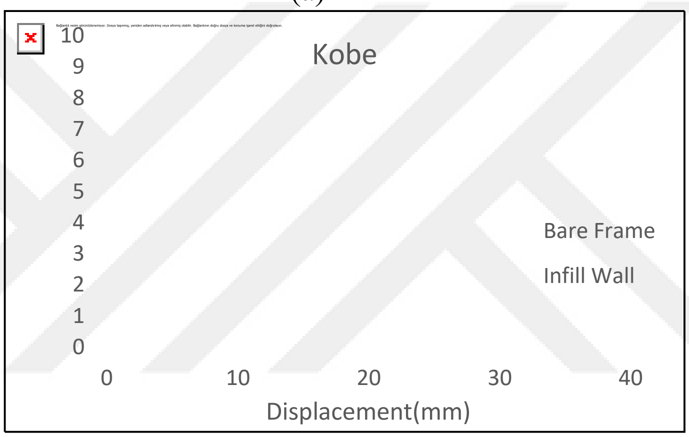

(b)

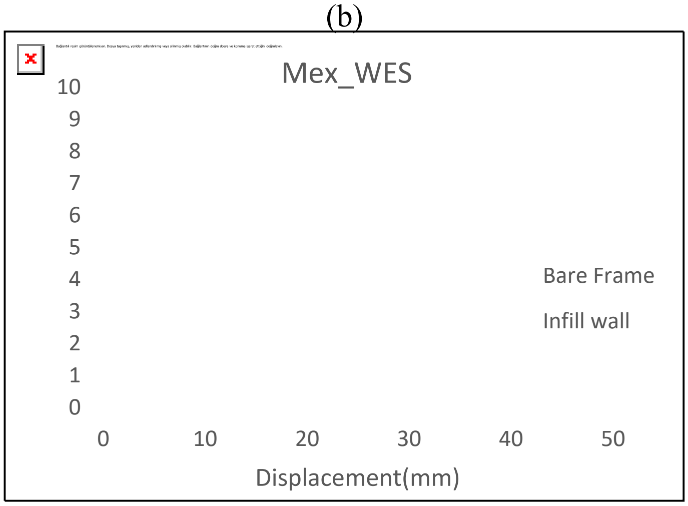

(c)

Figure 5.7: Maximum story displacement under a) El Centro, b) Kobe, and c) Mex_WES earthquakes.

Figure 5.8 shows the maximum displacement at each floor level for right-buildings (RB) of bare frame and infill wall cases. The highest roof displacement for the bare-frame case is 41mm,37mm, and 34mm under El Centro, Kobe, and Mex_WES earthquakes, respectively, while for infill wall case is 14mm, 15mm, and 13mm under El Centro, Kobe, and Mex_WES respectively. It has been decreased by 67.1%, 60%, and 62% under El Centro, Kobe, and Mex_WES earthquakes, respectively.

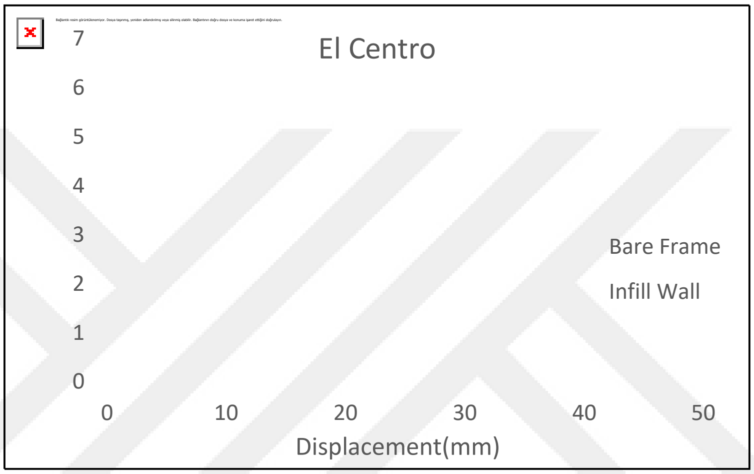

(a)

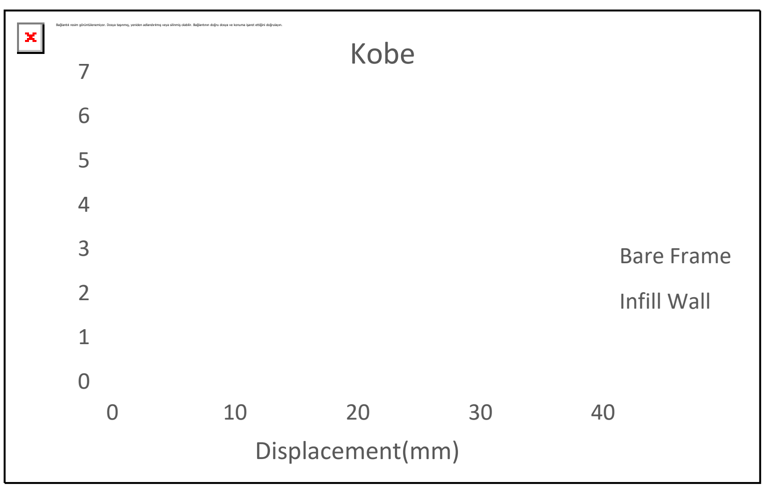

(b)

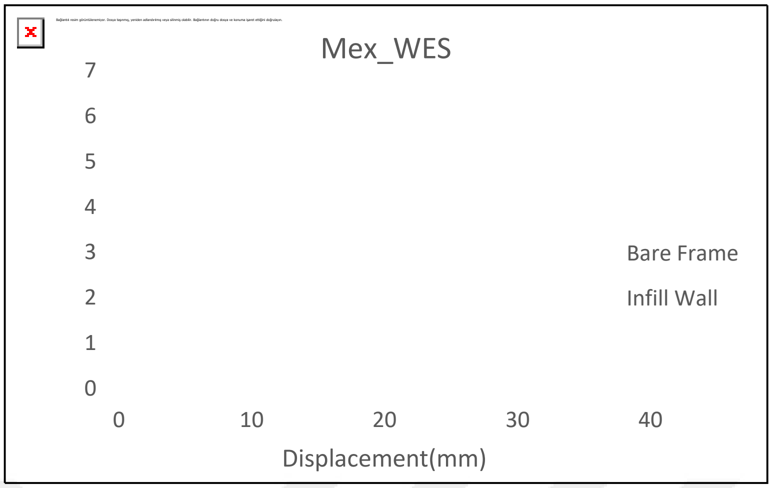

(c)

Figure 5.8: Maximum story displacement under a) El Centro, b) Kobe, and c) Mex_WES earthquakes.

5.2.3.2 Story Drift Ratio

Figure 5.9 shown the maximum drift ratio at each floor level for the left building. The highest drift ratio occurs at the middle floors were increased from the base up to the third floor, then started to decrease till roof level in case of the bare frame. For infill-wall case increased from base-level to the first floor only then started-to-decrease till reached to roof level.

The highest drift ratio for the bare frame's case is 0.26%, 0.21%, and 0.21% under El Centro, Kobe, and Mex_WES earthquakes, respectively, while for the infill wall case is 0.11%, 0.10%, and 0.11% under El Centro, Kobe, and Mex_WES earthquakes. It has been reduced by 56.7%, 53.2 %, and 49% under El Centro, Kobe, and Mex_WES earthquakes. The highest story drift ratio occurred at middle floors for both bare-frame and infill wall cases, respectively.

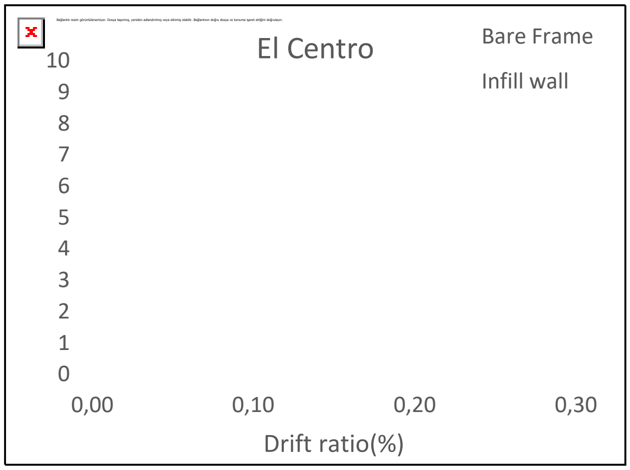

(a)

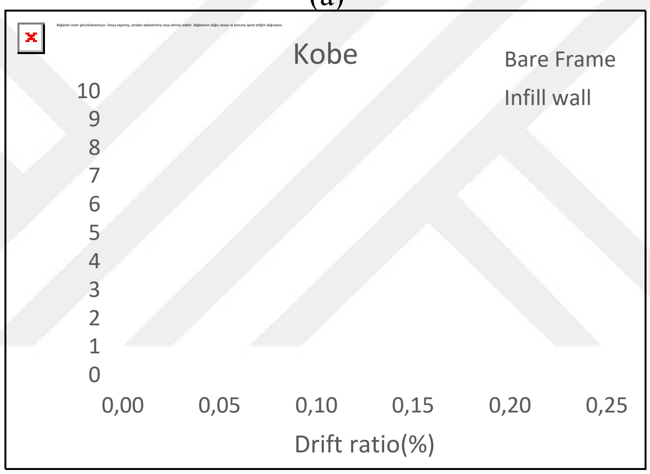

(b)

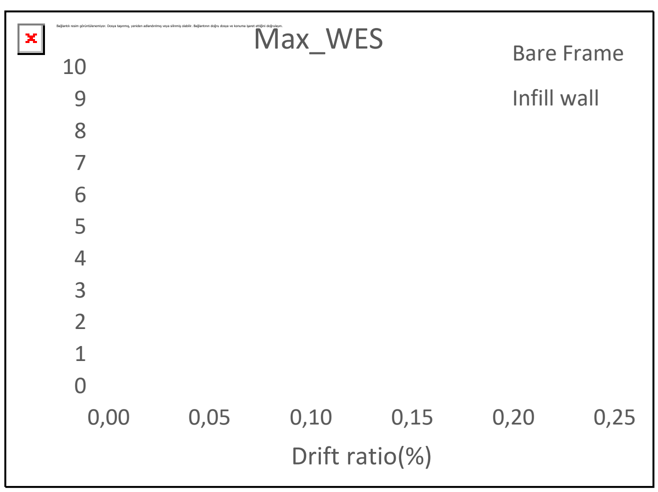

(c)

Figure 5.9: Maximum story drift ratio under a) El Centro, b) Kobe, and c) Mex_WES earthquakes.

Figure 5.10 shows the maximum story drift ratio of each floor for the right building. The highest story drift ratio has taken place on the middle floors of the building. The highest story drift ratio for the bare frame case is 0.33%, 0.29%, and 0.27% under El Centro, Kobe, and Mex_WES earthquakes, respectively, and for the infill wall case is 0.11%, 0.11%, and 0.09% under El Centro, Kobe, and Mex_WES earthquakes, respectively. It decreased by 68%, 63.3%, and 67.6% under El Centro, Kobe, and Mex_WES earthquakes, respectively. The highest points of the drift ratio occur at the second floor under all ground motions except the Kobe earthquake, which is taken place on the third floor, especially the bare frame one.

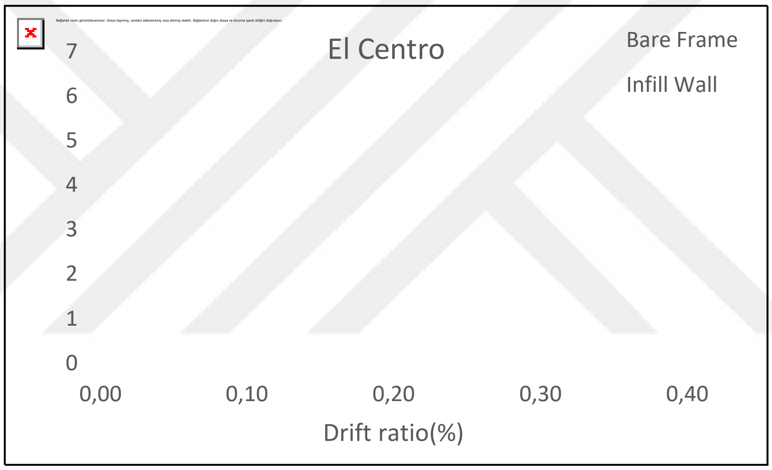

(a)

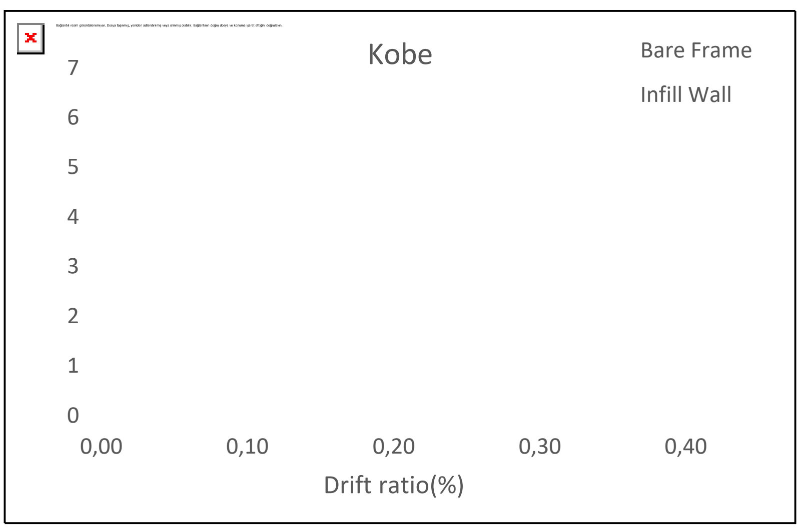

(b)

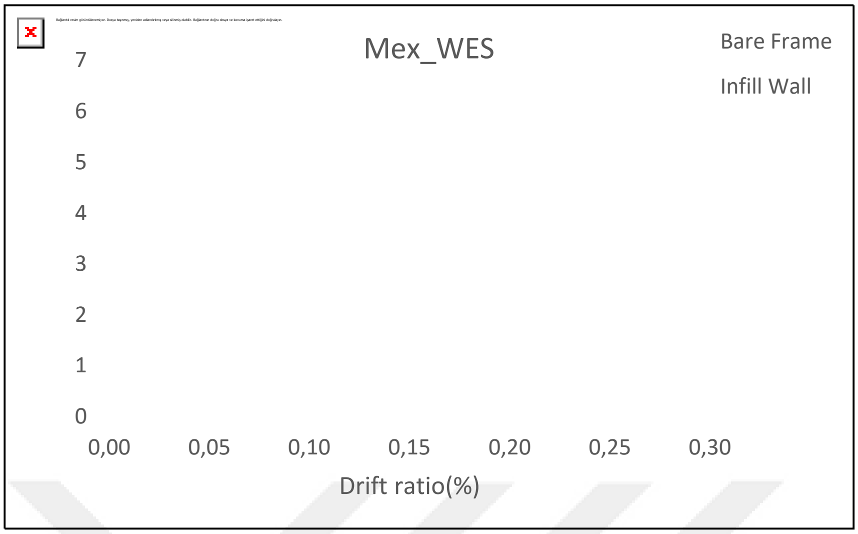

(c)

Figure 5.10: Maximum story drift ratio under a) El Centro, b) Kobe, and c) Mex_WES earthquakes.

5.2.3.3 Pounding Force

Figure 5.11 shows the pounding force at each floor level between adjacent buildings. The highest pounding force exists at the pounding level (sixth-floor level) under all ground motions for both cases.

The pounding force increased when increasing the difference between dynamics adjacent buildings (mass, stiffness, height, etc.). The highest pounding force for the bare-frame case is 576kN, 405kN, and 332kN and for the infill-wall case is 879kN, 669kN, and 783KN under El Centro, Kobe, and Mex_WES earthquakes, respectively.

The ratio between pounding force obtained from adjacent buildings with an infill wall to the bare frame's adjacent buildings is 1.52, 1.65, and 2.36 under El Centro, Kobe, and Mex_WES earthquakes.

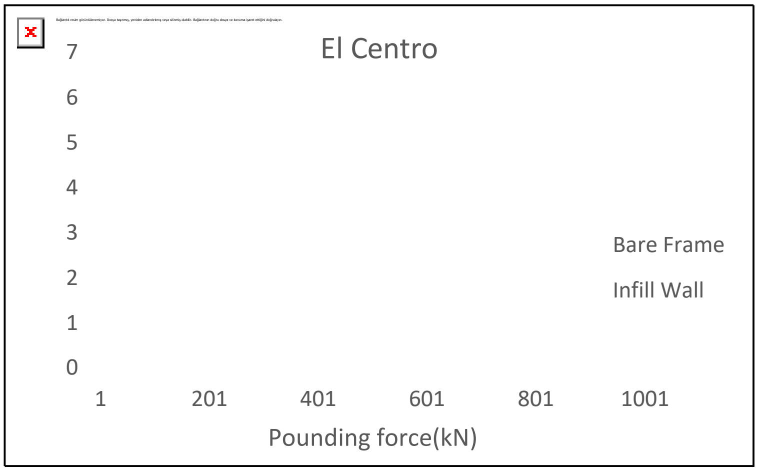

(a)

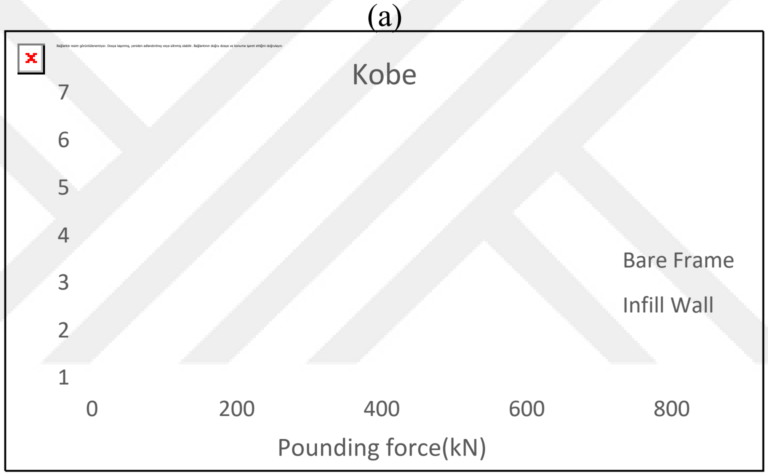

(b)

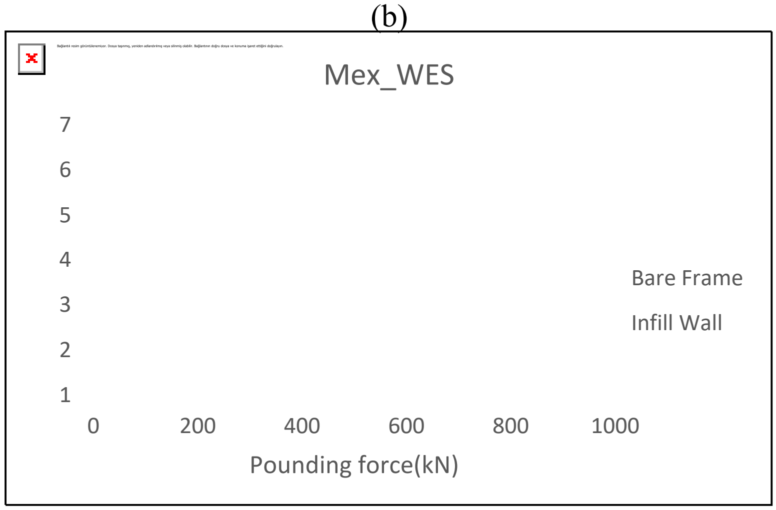

(c)

Figure 5.11: Maximum story drift ratio under a) El Centro, b) Kobe, and c) Mex_WES earthquakes.

5.2.3.4 Acceleration of Time History

An earthquake can cause high floor acceleration on the building due to the strong ground motion. Acceleration can be increased when the pounding between buildings increases. Table 5.5 shows the maximum acceleration at pounding level (sixth-floor level) for both cases under three different ground motions, particularly when the building moved toward the left side (L.S). The acceleration at the pounding level has been increased when the infill wall is adding to the building. The ratio between the infill wall to the bare frame case is 1-2 for the left building (L.B). Another hand ratio between the infill wall (full infilled) to the bare frame is 1.3.

Table 5.3: Maximum acceleration time history at pounding level.

	Ground Motion	Acceleration (L.S)		
		BF	IF	ratio (IF/BF)
L.B	El Centro	9.68	11.66	1.20
	Kobe	7.07	7.70	1.09
	Mex_WES	6.80	10.54	1.55
R.B	El Centro	19.33	31.91	1.65
	Kobe	14.91	18.33	1.23
	Mex_WES	9.52	24.36	2.56

All in unit m/s^2

Where L.S is left side direction, BF is the bare frame, IF infill wall framed, LB left building, and RB is right building.

Table 5.6 shown the maximum acceleration at pounding level for both cases of the adjacent building under various ground motions, especially when the building moved toward the right side (R.S). The acceleration increased when the pounding increased. However, the ratio between the infill wall to the bare frame case is 1-1.5 for the left building (L.B.). Another hand, the ratio between the infill wall (full infilled) to the bare frame is 1-2. Moreover, the acceleration of L.B. increased when the building moved to the left side, while the right building's acceleration increased when the building moved to the right side. Therefore, each building has been increased whenever it gets free space more than other directions.

Table 5.4: Maximum acceleration time history at pounding level.

	Ground Motion	Acceleration (R.S) BF	IF	ratio (IF/BF)
L.B	El Centro	4.05	4.94	1.22
	Kobe	3.47	3.98	1.15
	Mex_WES	3.55	3.88	1.09
R.B	El Centro	21.25	29.14	1.37
	Kobe	17.08	18.78	1.10
	Mex_WES	14.50	23.67	1.63

All in unit m/s^2

Where R.S is right side direction, BF is the bare frame, IF infill wall framed, LB left building, and RB is right building.

5.2.3.5 Pounding Force of Time History

Figure 5.12 show the pounding force-time history at the pounding level (6th floor) between adjacent building for both cases under different ground motions. The highest value of pounding force has taken place at the pounding level. The highest pounding force for the bare frame case is 576kN at 9.82s, and for the infill wall case is 879kN at 2.63s under the El Centro earthquake.

The highest pounding force for the bare frame reached 404.6kN at 15.15s, and for t infill wall is 669.16kN at 16.45s under the Kobe earthquake.

The highest pounding force for the bare frame is 313.8kN at 34.16s, and for the infill wall case is 782.73kN at 34.3s under Mex_WES. Thus, the pounding force has been increased whenever increase the dynamic behavior's difference between adjacent buildings.

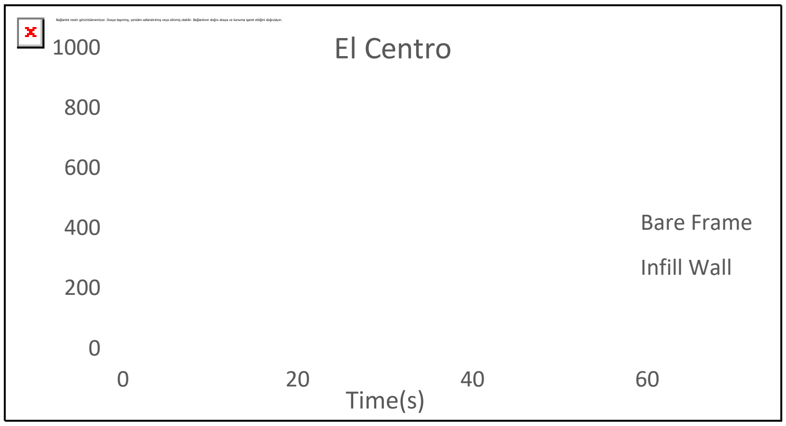

(a)

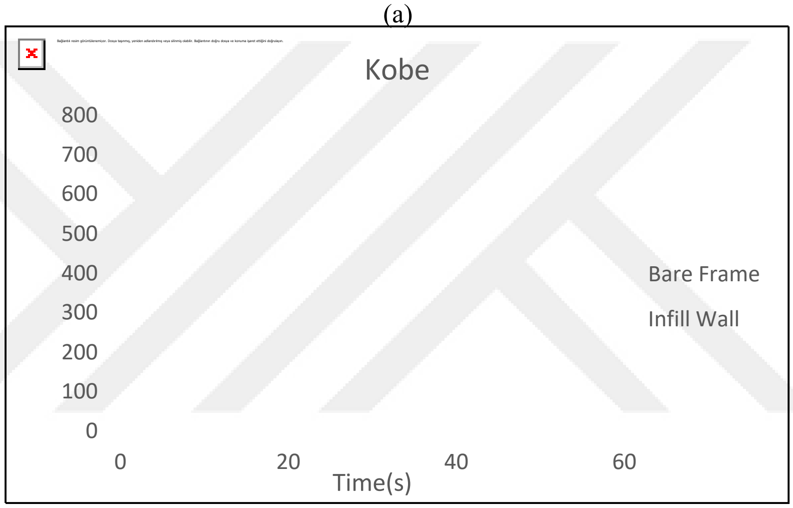

(b)

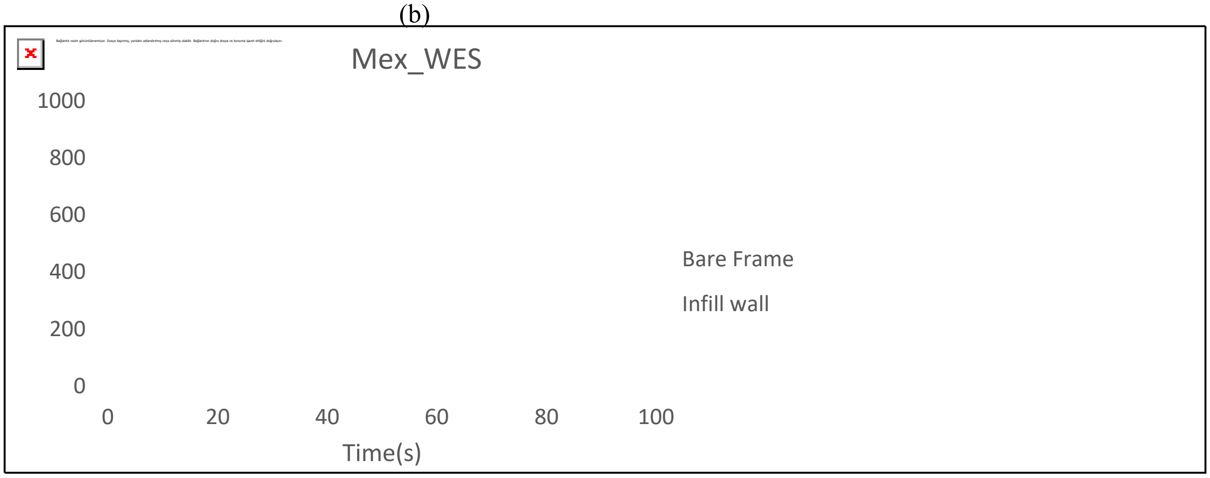

(c)

Figure 5.12: The pounding force of time history for a) El Centro, b) Kobe, and c) Mex_WES earthquakes.

5.2.3.6 Formation of Plastic Hinges

Figure 5.13 shows that the plastic hinge formed at the beams and columns on bare frame's adjacent buildings under the El Centro earthquake when it reaches maximum displacement of 46.48mm at 17.72sec. The hinges have appeared on the structure, such as the yielding stage (B). Therefore, the structural members have no failure and safe. However, the adjacent building with an infill wall has not appeared any plastic hinges due to the having infill wall, which has given more stiffness and cause reduce the displacement.

(b)

(b)

Figure 5.13: Plastic hinge formation for adjacent buildings with a) bare frame and b) infill wall.

CHAPTER 6

SUMMARY, CONCLUSIONS, AND RECOMMENDATIONS

6.1 Summary

Pounding or collision of adjacent buildings occurs when adjacent structures that have not enough separation distance between them during strong earthquake excitation. The reason for being the separation distance between adjacent buildings insufficient is financial as well as architectural issues. The only case of pounding events may happen when the adjacent structures move in a different direction, and the most reason is being their dynamic behavior differently. Several events related to pounding buildings have been observed during the last recent earthquakes. Influences from pounding buildings include low damages and severe damages, and at the same time, it may cause a complete collapse.

In this thesis, the 2D of RC frame adjacent buildings with the same floor level has been considered under five ground motions. The nonlinear elastic model simulated was considered with a constant gap separation distance. The adjacent buildings with different configurations such as bare frame' adjacent buildings and adjacent buildings with infill walls are studied. The adjacent buildings consist of nine and six stories. The suit input horizontal ground motions are between 0.20g to 0.25g and 6.0 to 7.2 of PGA and Mw.

The study has focused on assessing the influence of the adjacent buildings with bare frames only and with infill walls. In the high-impact case expression, the results obtained from both cases are compared. In addition, nonlinear time history analysis has been covered to find adequate results during the study. Initially, the results obtained from every single case for different ground motions are discussed. Finally, both cases are compared to determine the influence of pounding adjacent buildings with varying configurations under three ground motions. The final results have been selected to receive a permanent or partial solution for the pounding impact. The analysis task has been performed by SAP2000 software.

6.2 Conclusions

In this study, two different configurations for the RC of 2D pounding adjacent buildings are compared. These two different configurations of adjacent structures are bare frames adjacent buildings and adjacent buildings with infill walls. The results, including story displacements, story drifts, pounding forces, acceleration of time history, and pounding force of time history, are compared. The results obtained from this study summarized as follows: -

- Although the nonlinear time history analysis has been widely used as a perfect method to obtain results, it has been selected to perform this study using SAP2000.
- The story displacement for adjacent buildings having infill walls is less than those from adjacent buildings with bare frames only.
- For the left-building, the infill wall case, the displacement reduced by 53%, while the right-building of the infill wall case decreased by 67%.
- The story drift ratio for adjacent buildings having infill walls is less than those from adjacent buildings with bare frames only.
- For the left building of the infill wall, the drift ratio reduced by 57%, while the right building of the infill wall decreased by 68%.
- The infill wall provides more stiffness to the structure. Thus, it reduces the story displacement and story drift ratio.
- The highest pounding force occurs at the highest pounding level, but it may also appear on other floor levels.
- The pounding force for adjacent buildings having infill walls greater than those obtained from adjacent buildings with bare frames only.
- For the adjacent building having an infill wall, the pounding force increased 2.4 times.
- The pounding force increases when the difference of the dynamic behavior between adjacent buildings increases.

- The maximum acceleration at the pounding level of the adjacent building was having an infill wall greater than those obtained from adjacent buildings with bare frames only.
- The maximum acceleration increased by 1.6 times for the left building while the right building increased by 2.6 times.
- The acceleration for the right building increases when the building moves in the right direction. However, for the left building, the acceleration increases when the building moves toward the left side direction. Therefore, the acceleration increases when it freezes space.
- The acceleration increases whenever the pounding increase. Therefore, the acceleration for the adjacent buildings having infill walls higher than those obtained from the adjacent building with bare frame only.
- The plastic hinges have been appeared on the adjacent buildings with the bare frame, while they have been disappeared on the adjacent buildings with infill walls. Therefore, it indicates that the infill wall adds more stiffness to the system, reducing the displacement.
- The plastic hinge appeared on that the adjacent buildings have no failure and safer.
- The result i obtained from this study is very close to the results reached in the previous studies by many researchers.

The study results have shown that RC adjacent buildings are subjected to various horizontal ground motions near field regions. However, to evaluate the seismic response of Rc adjacent buildings during pounding, those different configurations (bare frame and infill wall) consider.

The results also indicate that the infill wall increases the difference between buildings' dynamic properties, which can cause to increase some response, such as pounding force and acceleration. In contrast, it causes to reduce others, such as displacement and drift ratio.

Therefore, the adjacent structures must be designed well to avoid the pounding during seismic by separating well by placing links between adjacent buildings, placing infill wall, adding a shear wall at the collision region, or adding bracing.

6.3 Recommendations

An experience obtained from the study and previous one; study has suggested that future researchers investigate this phenomenon considering the different aspects to reach a precise solution or reduce its effect. Thus, the following recommendations are suggested:

- Effect of pounding adjacent buildings with different floor levels (slab to column) during a seismic hazard.
- Effect of pounding of an irregular adjacent buildings during a seismic hazard.
- The study of the impact stiffness and the coefficient restitution on the adjacent pounding structures.
- Pounding adjacent buildings with shear wall consideration during earthquake excitation.
- The study of the minimum required separation between adjacent buildings from several different buildings codes.
- Study pounding adjacent buildings with soil-structure interaction consideration during an earthquake.
- Study pounding adjacent buildings with seismic isolation consideration during an earthquake.

REFERENCES

[1] Miari, Mahmoud, et al. "Seismic Pounding between Adjacent Buildings: Identification of Parameters, Soil Interaction Issues and Mitigation Measures." *Soil Dynamics and Earthquake Engineering*, vol. 121, no. 2, 2019, pp. 135–50.

[2] Abdel-Mooty, M., et al. "Modeling and Analysis of Factors Affecting Seismic Pounding of Adjacent Multi-Story Buildings." *WIT Transactions on the Built Environment*, vol. 104, 2009, pp. 127–38.

[3] Degg, M. R. "Some Implications of the 1985 Mexican Earthquake for Hazard Assessment." *Geohazards*, 1992, pp. 105–06.

[4] Scholl, Roger E. "Observations of the Performance of Buildings during the 1985 Mexico Earthquake, and Structural Design Implications." *International Journal of Mining and Geological Engineering*, vol. 7, no. 7, 1989, pp. 69–99.

[5] Kasai, Kazuhiko, and Bruce F. Maison. "Building Pounding Damage during the 1989 Loma Prieta Earthquake." *Engineering Structures*, vol. 19, no. 3, 1997, pp. 195–207.

[6] Jeng-Hsiang Lin, And Cheng-Chiang Weng. "A Study on Seismic Pounding Probability of Buildings in Taipei Metropolitan Area." *Journal of the Chinese Institute of Engineers, Transactions of the Chinese Institute of Engineers, Series A/Chung-Kuo Kung Ch'eng Hsuch K'an*, vol. 25, no. 2, 2002, pp. 123–35.

[7] Wibowo, Ari, et al. "*Damage in the 2008 China Earthquake*." 2008, pp. 01–08.

[8] Cole, Gregory, et al. "Interbuilding Pounding Damage Observed in the 2010 Darfield Earthquake." *Bulletin of the New Zealand Society for Earthquake Engineering*, vol. 43, no. 4, 2010, pp. 382–86.

[9] Romão, X.,et al. “Field Observations and Interpretation of the Structural Performance of Constructions after the 11 May 2011 Lorca Earthquake.” *Engineering Failure Analysis*, vol. 34, 2013, pp. 670–92.

[10]http://seismo.berkeley.edu/blog/2020/01/26/quake-in-turkey-highlights-the-hazard-in-the-east-bay.html

[11] Inel, Mehmet, et al. “Observations on the Building Damages after 19 May 2011 Simav (Turkey) Earthquake.” *Bull Earthquake Eng (2013)*, vol. 11, no. 1, 2013, pp. 255–83.

[12] Yazgan, Ufuk, et al. “Seismic Performance of Buildings during 2011 Van Earthquakes and Rebuilding Efforts.” *Journal of Earthquake Engineering and Engineering Vibration*, vol. 15, no. 3, 2016, pp. 591–606.

[13] Lin, Jeng-Hsiang and Weng, Cheng-Chiang. “Probability Analysis of Seismic Pounding of Adjacent Buildings.” *Earthquake Engineering and Structural Dynamics*, vol. 30, no. 10, 2001, pp. 1539–57.

[14] Garcia1, Diego Lopez. “Separation between Adjacent Nonlinear Structures for Prevention of Seismic Pounding.” *13th World Conference on Earthquake Engineering Vancouver*, no. 478, 2004, pp. 1–6.

[15] Khatami, S. M., et al. “Verification of Formulas for Periods of Adjacent Buildings Used to Assess Minimum Separation Gap Preventing Structural Pounding during Earthquakes.” *Advances in Civil Engineering*, 2019, pp. 1–8.

[16] Khatiwada, Sushil, et al. “An Experimental Study on Pounding Force between Reinforced Concrete Slabs.” *Proceeding of Australian Earthquake Engineering Society Conference*, 2013, pp. 1–9.

[17] Jankowski, Robert, et al. “Experimental Study on Pounding between Structures during Damaging Earthquakes.” *Key Engineering Materials*, vol. 627, 2015, pp. 249–52.

[18] Sołtysik, Barbara, et al. “Preventing of Earthquake-Induced Pounding between Steel Structures by Using Polymer Elements-Experimental Study.” *Procedia Engineering*, vol. 199, 2017, pp. 278–83.

[19] Jankowski, Robert. “Measuring Bias in Structural Response Caused by Ground Motion Scaling.” *Earthquake Engineering And Structural Dynamics*, vol. 39, no. 056, 2010, pp. 343–54.

[20] Shrestha, Bipin, et al. “Experimental Study of Seismic Pounding Effects on Bridge Structures Subjected to Spatially Varying Ground Motions.” *Australian Earthquake Engineering Society*, no. 11, 2014, pp. 1–9.

[21] Luo, Hexian, et al. “Research and Experiment on Optimal Separation Distance of Adjacent Buildings Based on Performance.” *Mathematical Problems in Engineering*, 2018, pp. 1–13.

[22] Guo, A. X., et al. “Experimental Study Of Highway Bridges With Pounding Effects Subject Bi-Directional Earthquake Excitations.” *14th World Conference on Earthquake Engineering (14WCEE)*, 2008, pp. 1–7.

[23] Jankowski, Robert. “Impact Force Spectrum for Damage Assessment of Earthquake-Induced Structural Pounding.” *Key Engineering Materials*, vol. 293–294, no. 9, 2005, pp. 711–18.

[24] Jankowski, Robert. “Pounding Force Response Spectrum under Earthquake Excitation.” *Engineering Structures*, vol. 28, no. 8, 2006, pp. 1149–61.

[25] Naderpour, H., et al. “Numerical Study on Pounding between Two Adjacent Buildings under Earthquake Excitation.” *Shock and Vibration*, 2016, pp. 1–9.

[26] Khatami, Seyed Mohammad, et al. “Determination of Peak Impact Force for Buildings Exposed to Structural Pounding during Earthquakes.” *Geosciences (Switzerland)*, vol. 10, no. 18, 2019, pp. 1–16.

[27] Jankowski, Robert. "Non-Linear Modelling of Earthquake Induced Pounding of Buildings." *Engineering Structures*, no. 8, 2004, pp. 12–13.

[28] Komodromos, Petros, et al. "Response of Seismically Isolated Buildings Considering Poundings." *Earthquake Engng Struct. Dyn.*, vol. 36, no. 5, 2007, pp. 1605–22.

[29] Mahmoud, Sayed, et al. "Earthquake-Induced Pounding between Equal Height Multi-Storey Buildings Considering Soil-Structure Interaction." *Bulletin of Earthquake Engineering*, vol. 11, no. 4, 2013, pp. 1021–48.

[30] López-Almansa, and Francisco And Kharazian, Alireza . "Parametric Study of Seismic Pounding between RC Buildings with Aligned Slabs." *Soil Dynamics and Earthquake Engineering*, vol. 8, 2014, pp. 1–12.

[31] Zou, Lihua, et al. " Seismic Pounding between Adjacent Buildings of Unequal Floor Height." *Journal of Vibroengineering*, vol. 16, no. 6, 2014, pp. 2756–67.

[32] Mate, N. U., Et Al. "Seismic Pounding Of Adjacent Linear Elastic Buildings With Various Contact Mechanisms For Impact Simulation." *Asian Journal of Civil Engineering (Bhrc)*, vol. 16, no. 3, 2015, pp. 383–415.

[33] Changhai, Zhai, et al. "Dimensional Analysis of Earthquake-Induced Pounding between Adjacent Inelastic MDOF Buildings." *Earthquake Engineering and Engineering Vibration*, vol. 14, no. 2, 2015, pp. 295–313.

[34] Abdel Raheem, Shehata E., et al. "Numerical Simulation of Potential Seismic Pounding among Adjacent Buildings in Series." *Bulletin of Earthquake Engineering*, vol. 17, no. 1, 2019, pp. 439–471.

[35] Jankowski, Robert, and Mahmoud, Sayed. *GeoPlanet : Earth and Planetary Sciences Earthquake- Induced Structural Pounding*. 2015, pp.1-155.

[36] Cole, G. L., et al. “Building Pounding State of the Art : Identifying Structures Vulnerable to Pounding Damage.” *2010 NZSEE Conference*, no. 11, 2010, pp.1–9.

[37] Albayrak, Uğur, et al. “An Overview of the Modelling of Infill Walls in Framed Structures.” *International Journal of Structural and Civil Engineering Research*, vol. 6, no. 1, 2017, pp. 24–29.

[38] Turkish Republic the Ministry of Public Works and Settlement, Turkish Earthquake Design Code TEC-2007, Ankara, Turkey, 2007.

[39] Budiwati, Ida Ayu Made, and Sukrawa Made. “Development of Diagonal Strut Width Formula for Infill Wall with Reinforced Opening in Modeling Seismic Behavior of RC Infilled Frame Structures.” *AIP Conference Proceedings*, vol. 1977, 2018, pp. 1–9.

[40] Murty, C. V. R., and Rupen Goswami. *Seismic Design Of Concrete Building Structures C.* 2003.

[41] AISC. Direct Analysis Method – Application and Examples. no. 9, 2017, pp. 1–66.

[42] Comparison Of The Analysis Methods For The Evaluation Of Local Second Order Effects In Concrete Structures – “ N Ominal Stiffness ” Method And “ N Ominal Curvature ” Method. 1992, pp. 1–19.

[43] https://www.simsolid.com/faq-items/material-properties/stress-strain-curve/

[44] Uruci, Rezarta. Effects Of Structural Irregularities On Low And Mid-Rise Rc Building Response. no. 6, 2016, pp.1-87

APPENDIX

Ground Motion Scaling Procedures

To obtain ground motion as scaling form, you have to follow the below steps: -

1. Design target response spectrum [see Figure 1].
2. Place the parameters of S_s, S_1, T_L, and site class [see Figure 2].
3. Upload the target RS to the PEER Ground Motion Database [see Figure 3].
4. Get the pre-scaled ground motion [see Figure 4].
5. Upload pre-scaled ground motion and target RS into the Seismomatch software [see Figure 5].
6. Match the pre-scaled ground motion with target RS [see Figure 6 and 7].
7. If the converging is a success, then download the matched ground motion acceleration and their RS.

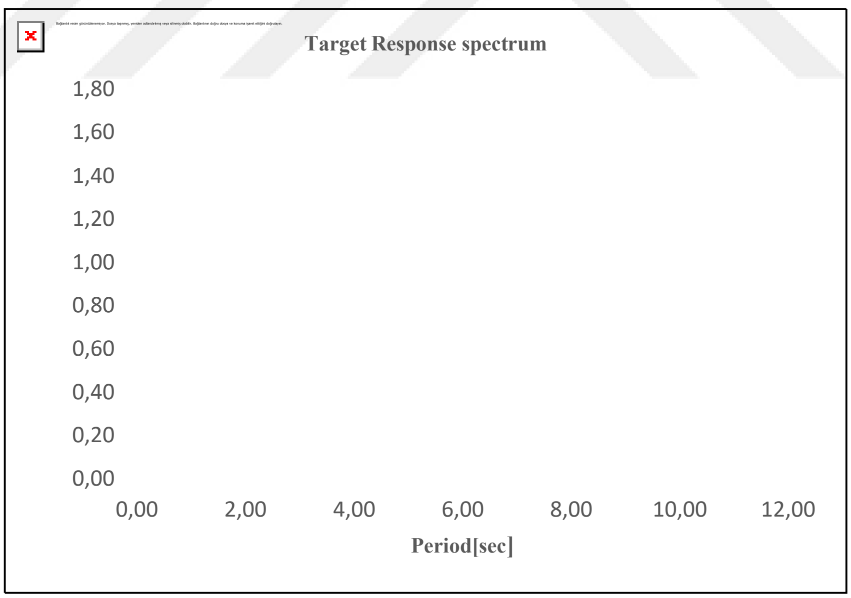

Figure 1: Design of target response spectrum

Figure 2: Applying Target RS on structure through SAP2000

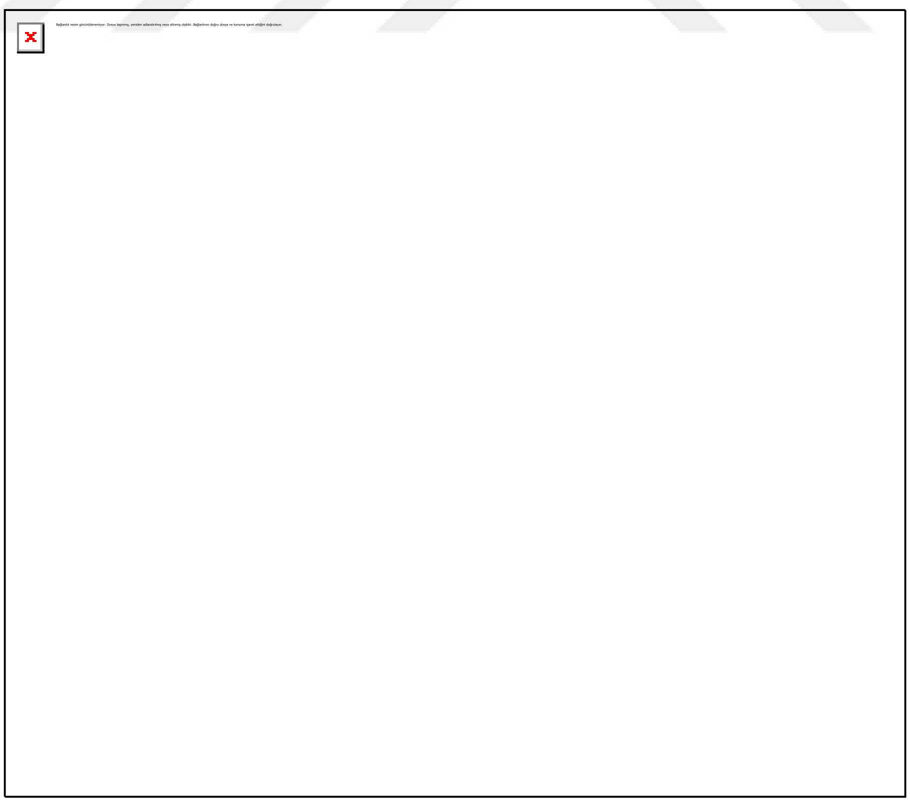

Figure 3: Uploading target RS to the PEER Ground Motion Database.

(a) Pre-scaled response spectrum (b) List of pre-scaled ground motions

Figure 4: Pre-scaled data from Peer ground motion database software

Figure 5: Success of Converging process.

Figure 6: Mean matching spectrum with Target RS.

Figure 7: Comparing original and matching of time series values.